NASA-RP-1155 19860015836

NASA
Reference
Publication
1155

December 1985

International Ultraviolet Explorer Atlas of O-Type Spectra From 1200 to 1900 Å

Nolan R. Walborn
Joy Nichols-Bohlin
Robert J. Panek

NASA Reference Publication 1155

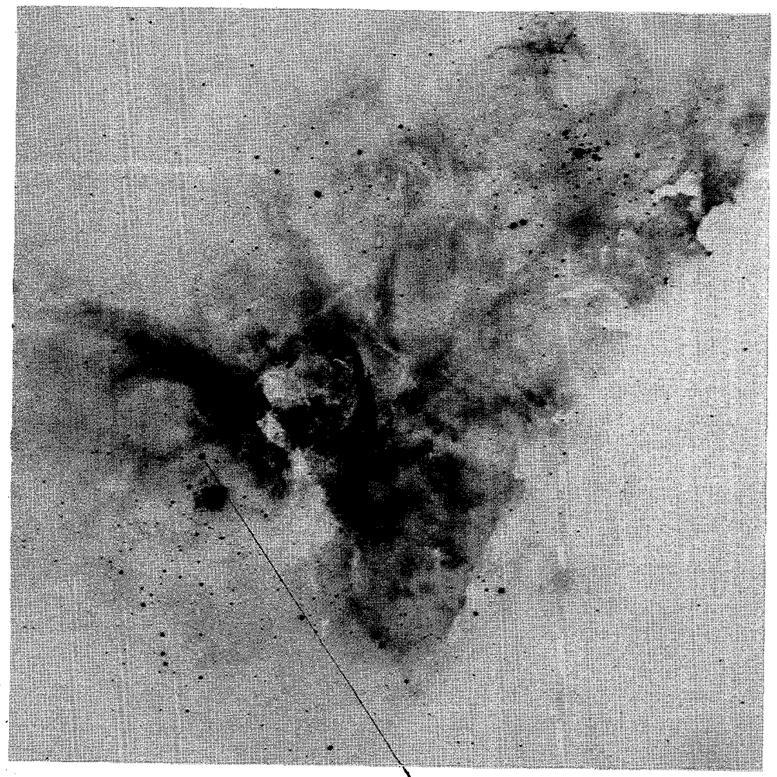

International Ultraviolet Explorer Atlas of O-Type Spectra From 1200 to 1900 Å

Nolan R. Walborn
Joy Nichols-Bohlin
Space Telescope Science Institute

Robert J. Panek
Raytheon Company and Wellesley College

Series Organizer: Jaylee M. Mead
Goddard Space Flight Center

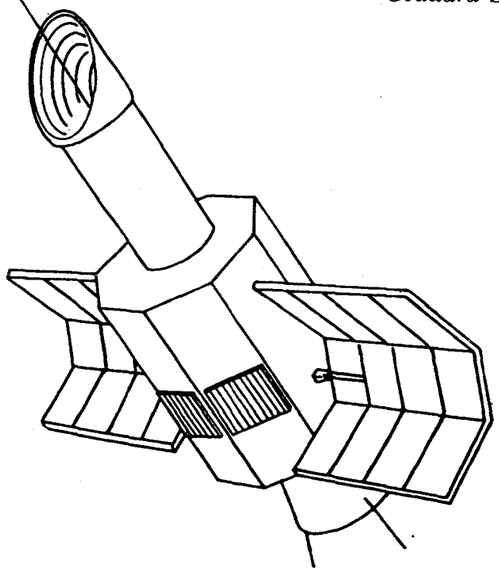

National Aeronautics
and Space Administration

Scientific and Technical Information Branch

1985

Library of Congress Cataloging-in-Publication Data
Walborn, Nolan R.
International ultraviolet explorer atlas of O-type spectra from 1200 to 1900 A.
(NASA RP ; 1155)
Bibliography: p. v
1. O stars—° Spectra—Atlases. 2. Spectrum, Ultraviolet—Atlases. 3. IUE (Artificial satellite)
I. Nichols-Bohlin, Joy. II. Panek, Robert J.
III. Mead, Jaylee M. IV. Title. V. Series: NASA reference publication ; 1155.
QB843.012W35 1985 523.8'7 85-15395

In my opinion, the classification should be based exclusively on a study of the spectra, i.e., of the *line and band absorption*, without reference to color, intrinsic brightness, and the like, much less to theoretical considerations. External considerations should be admitted only (1) in the search for differences, *perceptible in the spectra themselves*, which might otherwise escape notice; (2) in determining which of numerous small differences are entitled to specific rank.

. . . I would add the suggestion that a comparative study should be made of the spectra of stars of very different total luminosity but the same spectral class (Hertzsprung's "giant" and "dwarf" stars). If any definite and constant *spectroscopic* differences exist, they will be of value in classification.

H. N. Russell (1911)

INTRODUCTION

The primary purpose of this work is to investigate the existence of systematic trends in the ultraviolet line spectra of the O stars, including the prominent stellar wind features, and the degree to which they correlate with the optical spectral classifications. A subsidiary objective is to identify ultraviolet features which may themselves prove useful as classification criteria. The data archives of the International Ultraviolet Explorer (IUE) (Boggess *et al.* 1978) provide for the first time the combination of sample size, resolution, and homogeneity required for such an investigation of the O stars.

PHILOSOPHY

The approach adopted here is that enunciated by Russell in the above quotation, and pursued by Morgan (e.g., 1937) in the development of the MK system. The morphological methodology provides a powerful means to organize complex phenomena, show what is normal and what peculiar, and suggest (or eliminate) hypotheses. A key element is the separation of the description of the phenomena from their interpretation. In this way the uncertainties and assumptions inherent in the processes of measurement, calibration, and modeling are prevented from obscuring relationships which may exist among the phenomena, and which may subsequently provide vital guidance toward the ultimate objective of physical interpretation.

In concrete terms, no assumptions are made here about, for instance, reddening laws, gravities, or ionization fractions, which are required in order to derive such quantities as effective temperatures and mass-loss rates. Such analyses are, of course, essential for an eventual understanding of the ultraviolet spectra and the stellar winds, but it appears that the inevitable errors and approximations they involve may have hindered some previous efforts to establish relationships of the kind we seek. It is hoped that this work, by delineating more sharply the phenomenology of the ultraviolet spectral features, will contribute to future refinements in the physical interpretations.

DATA SELECTION

The wavelength region 1200-1900 Å corresponds to the high-quality range of the IUE short-wavelength camera and contains most of the interesting O-type spectral features accessible to IUE. The archives contain short-wavelength, high-resolution data for about 200 different O stars, of which we have examined 120. The primary selection criterion was the availability of homogeneous optical spectral classifications by Walborn (1972, 1973). In general, known interacting binaries and very rapid rotators were avoided, but a number of peculiar objects and categories which have been well described optically were specifically included. Table 1 lists the 101 spectrograms of 98 stars which are included in the atlas, together with the optical spectral classifications and the original IUE principal investigators.

DATA PROCESSING

The plots shown in this atlas were produced by resampling the standard IUE high-dispersion spectra to reduce the spectral resolution to a uniform 0.25 Å, and then normalizing the fluxes for convenient display of the spectral line features. This resolving power of 6000 at 1500 Å permits ready distinction between stellar and interstellar features in most O-type spectra. The original data consist of the gross spectrum and background from the merged, extracted spectral data file, which is the routine product of the IUE Spectral Image Processing System (IUESIPS) provided by the IUE observatories at Goddard Space Flight Center (GSFC) and Villafranca del Castillo (VILSPA). The IUESIPS data were retrieved from the tape copy of the IUE archive at GSFC, using routine procedures at the Regional Data Analysis Facility (RDAF). IUESIPS and its output products are described by Turnrose and Thompson (1984). The gross spectrum produced by IUESIPS consists of samples of the observed signal along each echelle order, integrated along a pseudo-slit; and a corresponding sample of the interorder background is provided. Each sample is tagged with its wavelength and with a data quality indicator. A major revision was made to IUESIPS on November 10, 1981 at GSFC and on March 11, 1982 at VILSPA. The primary effect for the plots in this atlas is the improved definition and registration of the extraction slit at the short-wavelength end of the spectrum, where the reduced cross-dispersion crowds the echelle orders. One symptom of poor placement of the extraction slit is negative flux in the core of Lyman alpha, which occurs when the background extraction includes a portion of the stellar signal in the adjacent order. It should be noted that all data shown in this atlas were acquired from the archive during the spring and summer of 1983.

Our first processing step was to compute the net spectrum by smoothing the background and subtracting it from the on-order signal. The second step was to correct for the systematic variation which is introduced along each order by the varying sensitivity of the echelle grating ("ripple" correction), and to discard overlap among the adjacent orders. The echelle

Table 1

Images Contained in the Atlas

HD/HDE/ BD/Sk	Name	Spectral Type	SWP	PI	Atlas Pages
108		O6:f?pe	13910	Conti	41-42
5005A		O6.5 V((f))	6135	York	31-32
12323		ON9 V	6503	Lester	37-38
12993		O6.5 V	16238	Dean	11-12
14633		ON8 V	4028	Jenkins	35-36
14947		O5 If+	10724	Conti	23-24
15558		O5 III(f)	8322	Underhill	15-16
15629		O5 V((f))	10754	Conti	9-10
19820		O8.5 III((n))	14632	Hilditch	17-18
24912	ξ Per	O7.5 III(n)((f))	3040	Stecher	15-16
30614	α Cam	O9.5 Ia	2591	Snow	7-8, 29-30, 39-40
34078	AE Aur	O9.5 V	2442	Vanden Bout	3-4
34656		O7 II(f)	15532	Bates	19-20
36486	δ Ori	O9.5 II	13471	Snow	7-8
36512	υ Ori	B0 V	3997	Humphries	3-4
36861	λ Ori	O8 III((f))	10611	Bates	17-18, 35-36
36879		O7 V(n)	4654	Wolff	33-34
			4699	Wolff	33-34
36960		B0.5 V	3577	Kamp	3-4
37022	Θ^1Ori C	O6-O4p var	14597	Panek	31-32
			14665	Bianchi	31-32
37043	ι Ori	O9 III	11164	Snow	17-18
37128	ε Ori	B0 Ia	6726	Jura	29-30
37742	ζ Ori	O9.7 Ib	2481	Vanden Bout	21-22
38666	μ Col	O9.5 V	6631	Jenkins	7-8
39680		O6 V:[n]pe var	16236	Dean	33-34
42088		O6.5 V	6908	Conti	31-32
46149		O8.5 V	6950	Conti	13-14
46150		O5 V((f))	10758	Conti	1-2
46202		O9 V	8845	Gull	13-14

Table 1 *continued*

Images Contained in the Atlas

HD/HDE/ BD/Sk	Name	Spectral Type	SWP	PI	Atlas Pages
46223		O4 V((f))	10757	Conti	1-2
46966		O8 V	6296	York	35-36
47839	15 Mon	O7 V((f))	13490	Snow	1-2
48279		O8 V	6504	Lester	35-36
48434		B0 III	6447	Lester	17-18
49798		sdO6	7664	McCluskey	33-34
53975		O7.5 V	8850	Gull	11-12
54662		O6.5 V	6299	York	31-32
66811	ζ Pup	O4 I(n)f	15296	Stalio	23-24
69464		O6.5 Ib(f)	10158	Westerlund	5-6
74194		O8.5 Ib(f)	5527	Wallerstein	21-22
91572		O6 V((f))	14743	Shull	11-12
91824		O7 V((f))	16533	Cowie	11-12
91969		B0 Ia	6510	Lester	29-30
92740		WN7-A	15131	Heckathorn	43-44
93028		O9 V	5521	Boksenberg	13-14
93129A		O3 If*	14007	Savage	23-24, 43-44
93130		O6 III(f)	6594	Hesser	15-16
93131		WN6-A	15132	Heckathorn	43-44
93146		O6.5 V((f))	11136	Hesser	5-6
93162		WN6-A	6609	Hesser	43-44
93204		O5 V((f))	7023	Conti	9-10
93250		O3 V((f))	14746	Shull	9-10
96715		O4 V((f))	7698	York	9-10
96917		O8.5 Ib(f)	7697	York	21-22
101190		O6 V((f))	6973	Conti	1-2
101413		O8 V	6971	Conti	13-14
101436		O6.5 V	6938	Conti	11-12
105056		ON9.7 Iae	14847	Lamers	39-40
112244		O8.5 Iab(f)	5167	Shull	25-26
122879		B0 Ia	9327	Carrasco	29-30

Table 1 *continued*

Images Contained in the Atlas

HD/HDE/ BD/Sk	Name	Spectral Type	SWP	PI	Atlas Pages
123008		ON9.7 Iab	16235	Dean	39-40
144470	ω^1Sco	B1 V	13906	Somerville	3-4
148937		O6.5f?p	9717	Bruhweiler	41-42
149038	μ Nor	O9.7 Iab	17396	Shull	27-28
149404		O9 Ia	9339	Hutchings	29-30
149438	τ Sco	B0.2 V	16222	calibration	33-34
151515		O7 II(f)	16113	Conti	19-20
151804		O8 Iaf	5140	Shull	25-26
151932		WN7-A	4334	Wilson	43-44
152249		OC9.5 Iab	6487	Lester	39-40
152405		O9.7 Ib-II	16215	Shull	19-20
152408		O8: Iafpe	14936	Snow	41-42
152424		OC9.7 Ia	9719	Bruhweiler	39-40
152590		O7.5 V	16098	Conti	13-14
162978		O7.5 II((f))	6038	York	19-20
163758		O6.5 Iaf	2892	Conti	5-6, 25-26
164794	9 Sgr	O4 V((f))	6040	York	9-10
167264	15 Sgr	O9.7 Iab	4368	Underhill	27-28
175754		O8 II((f))	9320	Carrasco	19-20
186980		O7.5 III((f))	6033	York	15-16
188001	9 Sge	O7.5 Iaf	3465	Sapar	25-26
188209		O9.5 Iab	6483	Lester	27-28
189957		O9.5 III	16234	Dean	7-8
190429A		O4 If+	4903	van Duinen	23-24
190864		O6.5 III(f)	10851	Shull	5-6
192639		O7 Ib(f)	9493	Boksenberg	21-22
193443		O9 III	18511	Gondhalekar	17-18
193514		O7 Ib(f)	18145	Boksenberg	21-22
201345		ON9 V	15004	Dufton	37-38
209975	19 Cep	O9.5 Ib	1424	Black	7-8
210809		O9 Iab	9103	Bruhweiler	27-28, 37-38

Table 1 *continued*

Images Contained in the Atlas

HD/HDE/ BD/Sk	Name	Spectral Type	SWP	PI	Atlas Pages
210839	λ Cep	O6 I(n)fp	14938	Snow	25-26
214680	10 Lac	O9 V	17394	Shull	3-4, 37-38
218915		O9.5 Iab	9322	Carrasco	27-28
269698	(LMC)	O4 If+	6967	Conti	23-24
			8011	Willis	23-24
269810	(LMC)	O3 III(f*)	10755	Conti	15-16
303308		O3 V((f))	9015	Underhill	1-2
+60°2522		O6.5(n)(f)p	8840	Johnson	41-42
Sanduleak 80	(SMC)	O7 Iaf+	6564	Savage	41-42

ripple is the only component of the instrumental sensitivity function which affects the appearance of spectral line features. Its removal is necessary to obtain undistorted profiles of the strongest lines, and to prevent discontinuities at the junctions between orders. These first two processing steps were performed with standard software available at the RDAF. The ripple correction is based on the calibration by Ake (1981). Any error in the ripple correction tends to show first at the longest wavelengths. Overlap among adjacent orders is discarded beyond the wavelengths at which the sensitivities are equal. These wavelengths are recorded for subsequent display with each spectrum (see below).

The third processing step was to resample the spectrum to 0.25 Å resolution, and to splice the adjacent orders. Each original sample was considered an estimate of the flux averaged over a bin whose width was equal to the spacing between the adjacent points. Each new sample was computed as a weighted average of the original samples; the weight of each original sample is equal to the fraction of its bin which falls within the 0.25 Å window centered on the new wavelength point. However, the weight is zero for any original point for which the IUESIPS quality factor indicated contamination by a camera reseau, saturation of the vidicon camera, or a particle radiation hit. The new sample points were spaced evenly at 0.25 Å intervals from 1150 Å to 1950 Å. For each new sample point, a quality factor was computed as the sum of the weights for the original samples contributing to the new point. This quality factor ranges from about 6 at 1200 Å (when there is no effect of a reseau, etc.) to about 4 at 1800 Å, for IUESIPS processing at GSFC before November 1981. With the newer version of IUESIPS, this factor is roughly doubled due to the finer wavelength sampling of the spectrum. The quality factor is shown, rescaled, with each spectral plot in the atlas.

The final processing step was to rescale the resampled spectrum to locate the stellar continuum approximately at a uniform level. This last step was performed interactively by R.J.P., by identifying about a dozen "continuum" points spaced along the interval 1150-1950 Å. Then, the flux was divided by a cubic spline interpolated through these points. The intention here was not to precisely define a stellar continuum; it was simply to place the spectrum onto a convenient scale for plotting over the full spectral range. The renormalization

function usually showed a broad hump between 1400 and 1600 Å. It is unclear whether this represents a rise in the instrumental sensitivity near 1500 Å or an effect of blended spectral absorption features near 1400 and 1600 Å. Similarly, the data quality factor was normalized to remove the effect of the decreasing spectral dispersion toward longer wavelengths, which causes the number of original samples within a constant 0.25 Å window to decrease. The third and the final processing steps were performed with the facilities of the RDAF by means of software newly written for these purposes.

The resulting spectrograms, data quality factors, and order splice points were plotted on a Model 1055 Calcomp plotter, at a scale of 10 Å/cm. The spatial registration of this plotter was found to be very precise and reproducible. Narrow positive spikes in the flux data due to particle radiation hits and the geocoronal Lyman alpha emission were eliminated manually at the final plotting stage.

These plots are reproduced in the atlas in montages of four or five spectrograms. Wavelength intervals of 10 Å are marked by the ticks along the horizontal lines, which also give the zero level for the spectrogram immediately above. Each echelle order splice point is marked by an "X" on the zero level line. The span of an echelle order increases from about 10 Å at 1200 Å to about 25 Å at 1800 Å. The data quality factor is shown above each stellar spectrogram. It has been offset vertically so that its zero level occurs above the flux zero level, at 7/8 the vertical distance to the top. Small downward spikes in the data quality factor occur where a few of the original sample points in the 0.25 Å resample window were contaminated by a reseau. Large downward spikes occur where most or all of the points were affected by a reseau. In many cases, no effect of the reseau is apparent in the stellar spectrum; this occurs when the reseau falls close to but not precisely onto the stellar spectrum, and the interorder background is weak.

THE ATLAS

The atlas is arranged in the 22 montages listed in Table 2, each containing four or five spectrograms. As the table indicates, the atlas may be divided into three broad sections. The first four montages provide an overview consisting of the main sequence from O3 through B1, followed by luminosity sequences at O6.5 and O9.5. The second section presents an extensive sample of normal spectra, organized into restricted spectral-type ranges at fixed luminosity classes, establishing that the characteristics of the overview spectra are indeed representative of their types, and demonstrating their development as a function of spectral type at all luminosity classes. The final section of the atlas illustrates various categories of peculiar spectra. All of the spectral types shown are prior optical classifications; the high degree of correlation between the ultraviolet spectra, including the stellar wind features, and the optical classifications is immediately apparent.

The principal interstellar lines are marked in the spectrum of HDE 303308 in the first montage, and they are listed in Table 3.

The salient features of each montage are briefly discussed in a column of text at the left. These columns contain numerical references to earlier optical studies of the same stars, which are identified in the reference list at the end of this discussion.

Table 2
Outline of the Atlas

Montage Title	Pages
A. Normal Spectra: Overview	
O3-O7 Main Sequence	1-2
O9-B1 Main Sequence	3-4
Luminosity Effects at O6.5	5-6
Luminosity Effects at O9.5	7-8
B. Normal Spectra: Sample	
Early O Dwarfs	9-10
Middle O Dwarfs	11-12
Late O Dwarfs	13-14
Early O Giants	15-16
Late O Giants	17-18
Bright Giants	19-20
Ib Supergiants	21-22
Early Of Supergiants	23-24
Middle Of Supergiants	25-26
Iab Supergiants	27-28
Ia Supergiants	29-30
C. Peculiar Spectra	
Weak Winds	31-32
Peculiar Dwarfs	33-34
Nitrogen Enhanced O8 Dwarfs	35-36
Nitrogen Enhanced O9 Dwarfs	37-38
ON/OC Supergiants	39-40
Peculiar Giants/Supergiants	41-42
The WN-A Stars	43-44

DISCUSSION

The dominant conclusion from this atlas is that the ultraviolet spectra of the majority of O stars, including their prominent stellar wind features, display strong systematic trends and a high degree of correlation with the optical spectral classifications. The Si IV luminosity effect, the main-sequence phenomena, and the ON/OC stars have been discussed in more detail by Walborn and Panek (1984a,b; 1985), respectively. The Of and WN-A sequences provide further examples of remarkably detailed correspondences between stellar wind features and optical spectral types, not discussed previously. In view of the spectral-type calibrations, these relationships imply that O-type winds are governed by the fundamental stellar parameters, and they strongly constrain physical theories for the origin of the winds in that direction.

The question of variability in individual ultraviolet spectra has not been addressed here,

Table 3
Principal Interstellar Lines

Species	λ (Å)	Species	λ (Å)
S II	1250.6	Si II	1526.7
S II	1253.8	C IV	1548.2
S II	1259.5	C IV	1550.8
Si II	1260.4	C I	1560
Si II*	1264.7	Fe II	1608.5
C I	1277	C I	1657
C I	1280	Al II	1670.8
O I	1302.2	Ni II	1709.6
Si II	1304.4	Ni II	1741.5
C I	1329	Si II	1808.0
C II	1334.5	Al III	1854.7
C II*	1335.7	Al III	1862.8
Ni II	1370.1		
Si IV	1393.8		
Si IV	1402.8		

except in a few cases. Numerous studies have described such variations in sharp wind absorption components and in profile shapes, but they are small relative to the morphological trends shown here. Indeed, the atlas as a whole demonstrates that point, since if it were otherwise, these trends and relationships would not be observed.

The *Copernicus* atlas of Snow and Morton (1976) shows that the behavior with luminosity of the C III λ1176 stellar wind effect is strikingly similar to that of the Si IV shown here. The ionization potentials of these two species are very similar (48 and 45 eV, respectively), while those of C IV, N IV, and N V, which show wind effects on the main sequence, are significantly higher (64, 78, and 98 eV). When modeled in detail, these effects should improve our knowledge of the physical conditions in these winds.

N.R.W. wishes to acknowledge Jim Hesser's enthusiasm for trying out new techniques, and Ted Gull's support of an extended visit to the Goddard Space Flight Center, which were contributing factors toward this undertaking. N.R.W. was a National Research Council Senior Associate in the Laboratory for Astronomy and Solar Physics at GSFC when this work was begun.

This project was greatly facilitated by the easy access to the IUE archive at the GSFC Regional Data Analysis Facility. All data processing was performed with the computing and plotting facilities of the RDAF, mostly during idle time overnight. The staff of the RDAF cooperated by providing assistance when it would not interfere with other users of the facility. Support was provided by NASA IUE grant NAS 5-25774 to program OBGNW.

REFERENCES

Abbott, D. C., Bohlin, R. C., and Savage, B. D. 1982, *Ap. J. Suppl.*, **48**, 369.
Ake, T. B., III 1981, *IUE NASA Newsletter*, No. 15, p. 60.
Bashkin, S. and Stoner, J. O., Jr. 1978, *Atomic Energy-Level and Grotrian Diagrams, Vol. 1, Hydrogen I–Phosphorus XV. Addenda* (Amsterdam: North-Holland), p. 86.
Boggess, A., Carr, F. A., Evans, D. C., Fischel, D., Freeman, H. R., Fuechsel, C. F., Klinglesmith, D. A., Krueger, V. L., Longanecker, G. W., Moore, J. V., Pyle, E. J., Rebar, F., Sizemore, K. O., Sparks, W., Underhill, A. B., Vitagliano, H. D., West, D. K., Macchetto, F., Fitton, B., Barker, P. J., Dunford, E., Gondhalekar, P. M., Hall, J. E., Harrison, V. A. W., Oliver, M. B., Sandford, M. C. W., Vaughan, P. A., Ward, A. K., Anderson, B. W., Boksenberg, A., Coleman, C. I., Snijders, M. A. J., and Wilson, R. 1978, *Nature*, **275**, 372.
Bruhweiler, F. C., Kondo, Y., and McCluskey, G. E. 1981, *Ap. J. Suppl.*, **46**, 255.
Hamann, W.-R., Gruschinske, J., Kudritzki, R. P., and Simon, K. P. 1981, *A. and Ap.*, **104**, 249.
Klein, R. I. and Castor, J. I. 1978, *Ap. J.*, **220**, 902.
Kudritzki, R. P. and Simon, K. P. 1978, *A. and Ap.*, **70**, 653.
Morgan, W. W. 1937, *Ap. J.*, **85**, 380.
Russell, H. N. 1911, *Ap. J.*, **33**, 292.
Snow, T. P., Jr. and Morton, D. C. 1976, *Ap. J. Suppl.*, **32**, 429.
Turnrose, B. E. and Thompson, R. W. 1984, *International Ultraviolet Explorer Image Processing Information Manual, Version 2.0* (Computer Sciences Corporation TM-84/6058).
Walborn, N. R. 1970, *Ap. J. Letters*, **161**, L149 (reference 1).
———. 1971, *Ap. J. Letters*, **167**, L31 (reference 2).
———. 1971, *Ap. J. Suppl.*, **23**, 257 (reference 3).
———. 1972, *A. J.*, **77**, 312.
———. 1973, *A. J.*, **78**, 1067 (reference 4).
———. 1974, *Ap. J.*, **189**, 269 (reference 5).
———. 1976, *Ap. J.*, **205**, 419 (reference 6).
———. 1977, *Ap. J.*, **215**, 53 (reference 7).
———. 1980, *Ap. J. Suppl.*, **44**, 535 (reference 8).
———. 1981, *Ap. J. Letters*, **243**, L37 (reference 9).
———. 1982, *Ap. J. Letters*, **254**, L15 (reference 10).
———. 1982, *Ap. J.*, **256**, 452 (reference 11).
Walborn, N. R. and Panek, R. J. 1984a, *Ap. J. Letters*, **280**, L27.
———. 1984b, *Ap. J.*, **286**, 718.
———. 1985, *Ap. J.*, **291**, 806.
Wiese, W. L., Smith, M. W., and Glennon, B. M. 1966, *Atomic Transition Probabilities, Vol. 1, Hydrogen Through Neon* (Washington, D.C.: GPO), pp. 73-74.

O3-O7

MAIN SEQUENCE

These stars are the primary optical classification standards for their types. The ultraviolet spectral features, both stellar-wind and photospheric, are strongly correlated with the optical spectral types.

N V λλ1239,1243 and C IV λλ1548,1551 have saturated P Cyg profiles from O3 through O6, which decline at O7 (note the strong, sharp, displaced wind absorption components in 15 Mon). The unsaturated, subordinate line N IV λ1718 behaves analogously. O V λ1371 is an asymmetrical absorption feature from O3 to O6. In contrast, Si IV λλ1394,1403 shows no stellar-wind effect anywhere on the main sequence.

The ratio Fe V λ1429/λ1430 provides a useful ultraviolet classification criterion, declining from unity between O4 and O5. The increased strength and ratio of N III λλ1748,1752 discriminate O4 from O3. The majority of photospheric absorption lines in this region of O-type spectra are due to Fe V below 1500 Å and to Fe IV above (Bruhweiler, Kondo, and McCluskey 1981).

The strongest interstellar lines are marked by dots in the spectrum of HDE 303308 (see Table 3 with the introductory text).

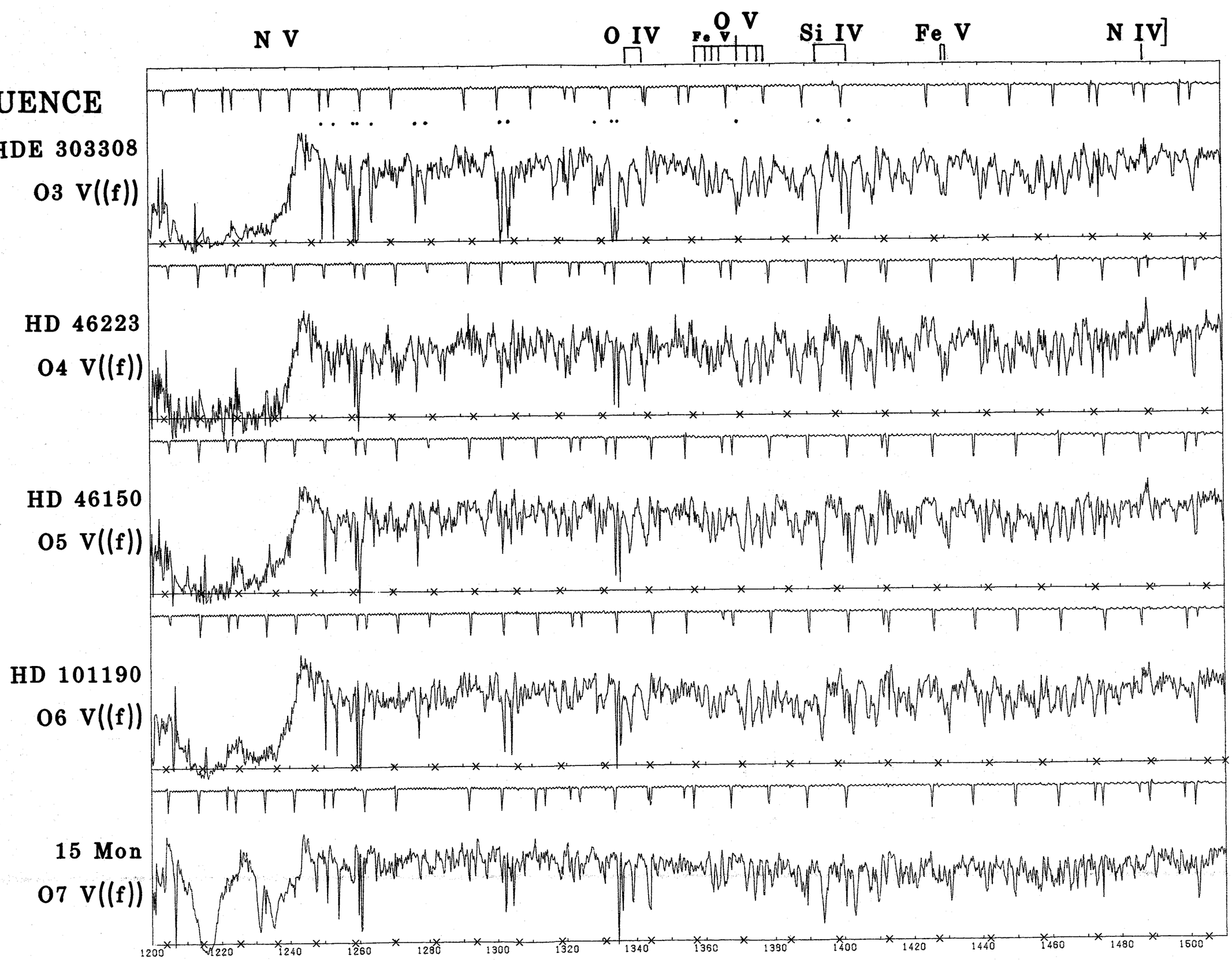

C IV λ1574 He II Fe IV N IV N III

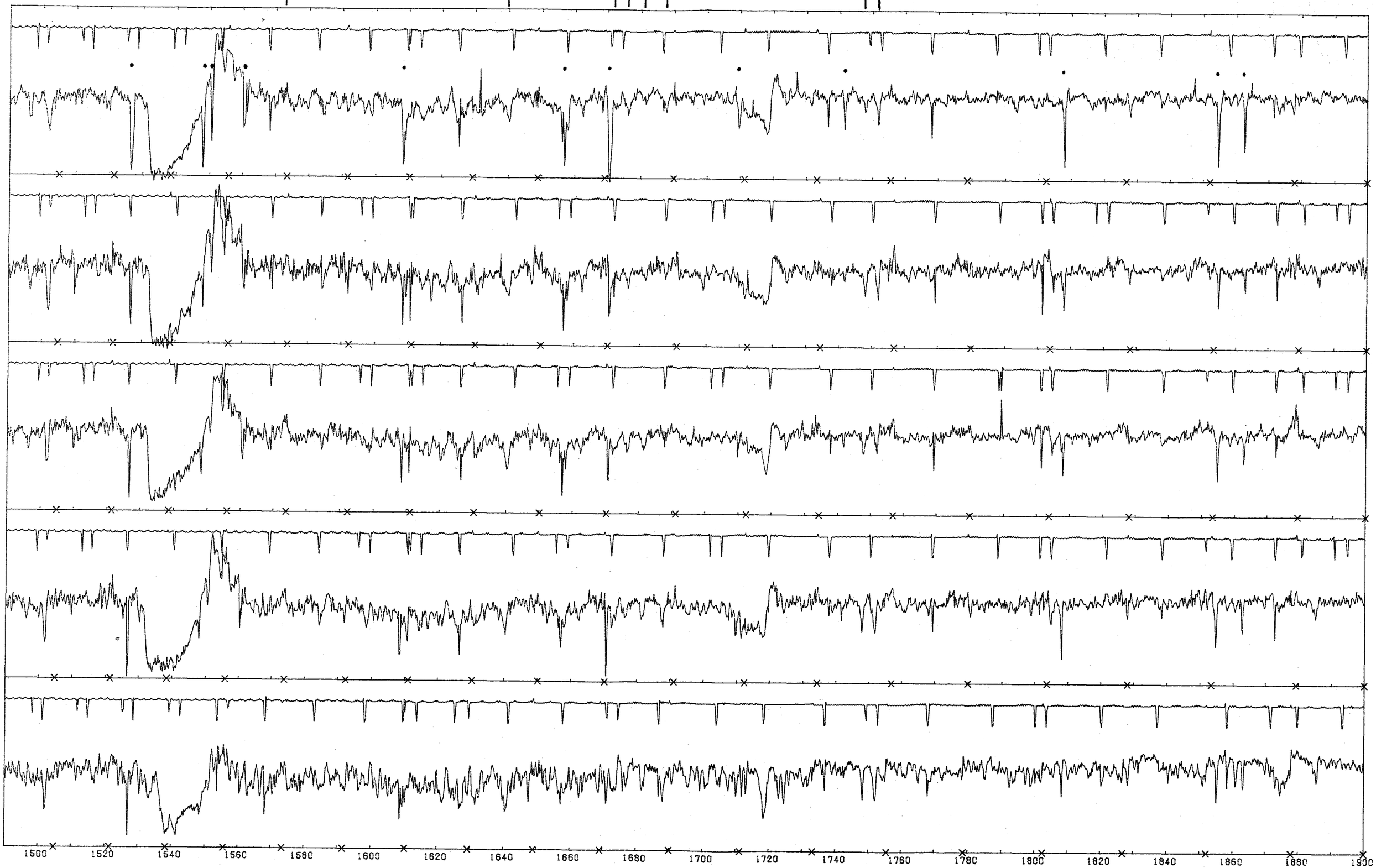

O9-B1

MAIN SEQUENCE

These stars are the primary optical classification standards for their types. The ultraviolet spectral features, both stellar-wind and photospheric, are strongly correlated with the optical spectral types.

C IV λλ1548,1551 declines gradually from a strong wind absorption trough at O9 to pure photospheric (plus interstellar) absorption at B1. Si IV λλ1394,1403 shows no stellar-wind effect in any normal main-sequence spectra.

C III λλ1426,1428 strengthen relative to Fe V λ1430, providing a useful ultraviolet classification criterion.

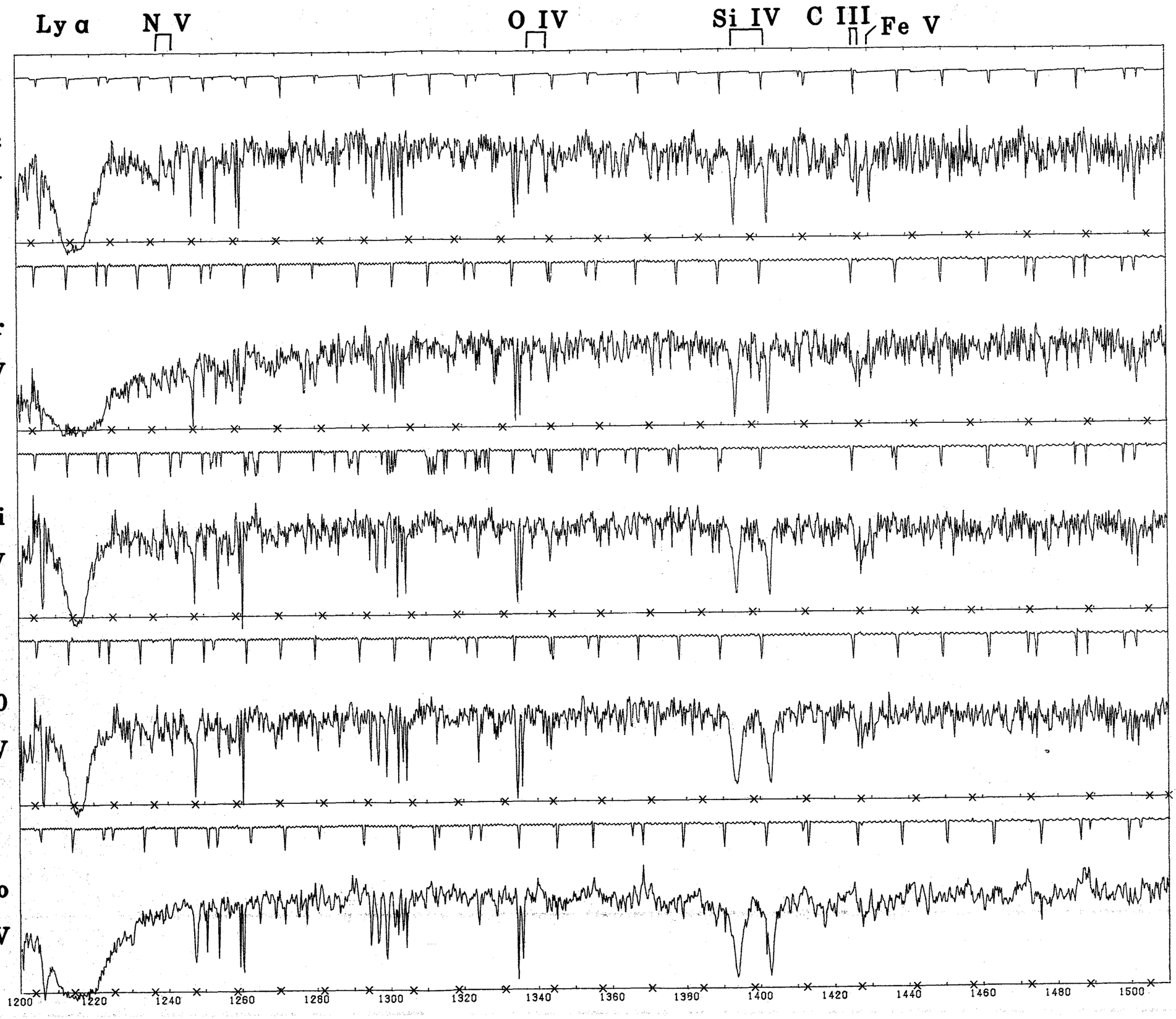

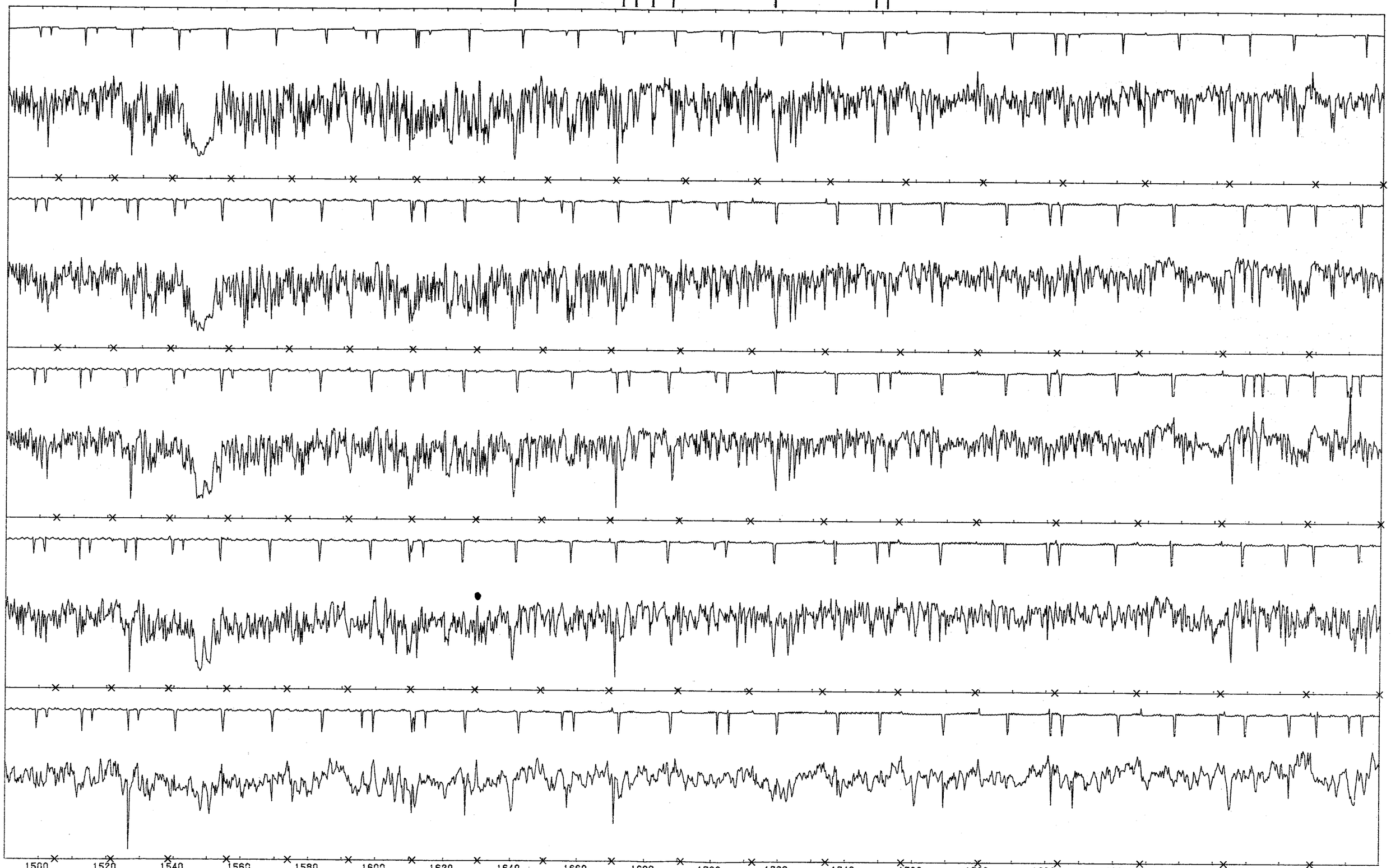
C IV
He II
Fe IV
N IV
N III
1500
1520
1540
1560
1580
1600
1620
1640
1660
1680
1700
1720
1740
1760
1780
1800
1820
1840
1860
1880
1900

LUMINOSITY EFFECTS AT O6.5

An analogous montage of blue-violet spectrograms, illustrating the different degrees of the f-parameter, is given by Walborn (1973).

The N V λλ1239,1243 and C IV λλ1548,1551 profiles show that all of these stars have strong stellar winds. Sharp shortward wind absorption components are prominent in HD 93146.

In contrast, the stellar-wind effect in Si IV λλ1394,1403 displays a pronounced luminosity dependence, with no effect at class V, and a gradual development through the intermediate classes to a full P Cyg profile at Iaf.

The emission line at λ1574 may be due to an N III transition with the same lower level as the optical Of lines λλ4634-4640-4642 (Bashkin and Stoner 1978), or alternatively to a predicted [N IV] transition (Wiese, Smith, and Glennon 1966).

He II λ1640 is in absorption in the f and (f) spectra, i.e., with λ4686 in emission or neutralized, respectively, at this type, consistent with the models of Klein and Castor (1978).

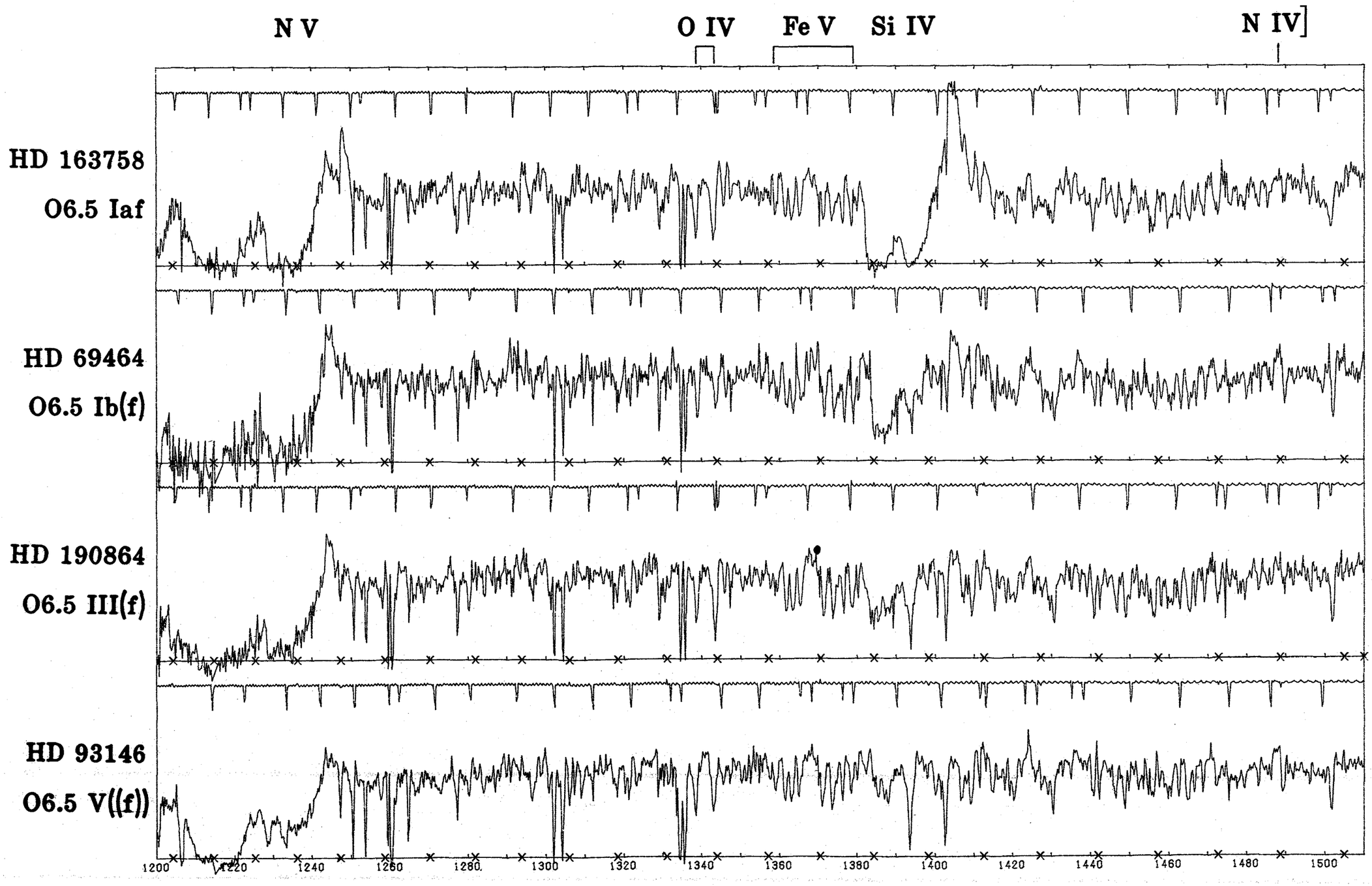

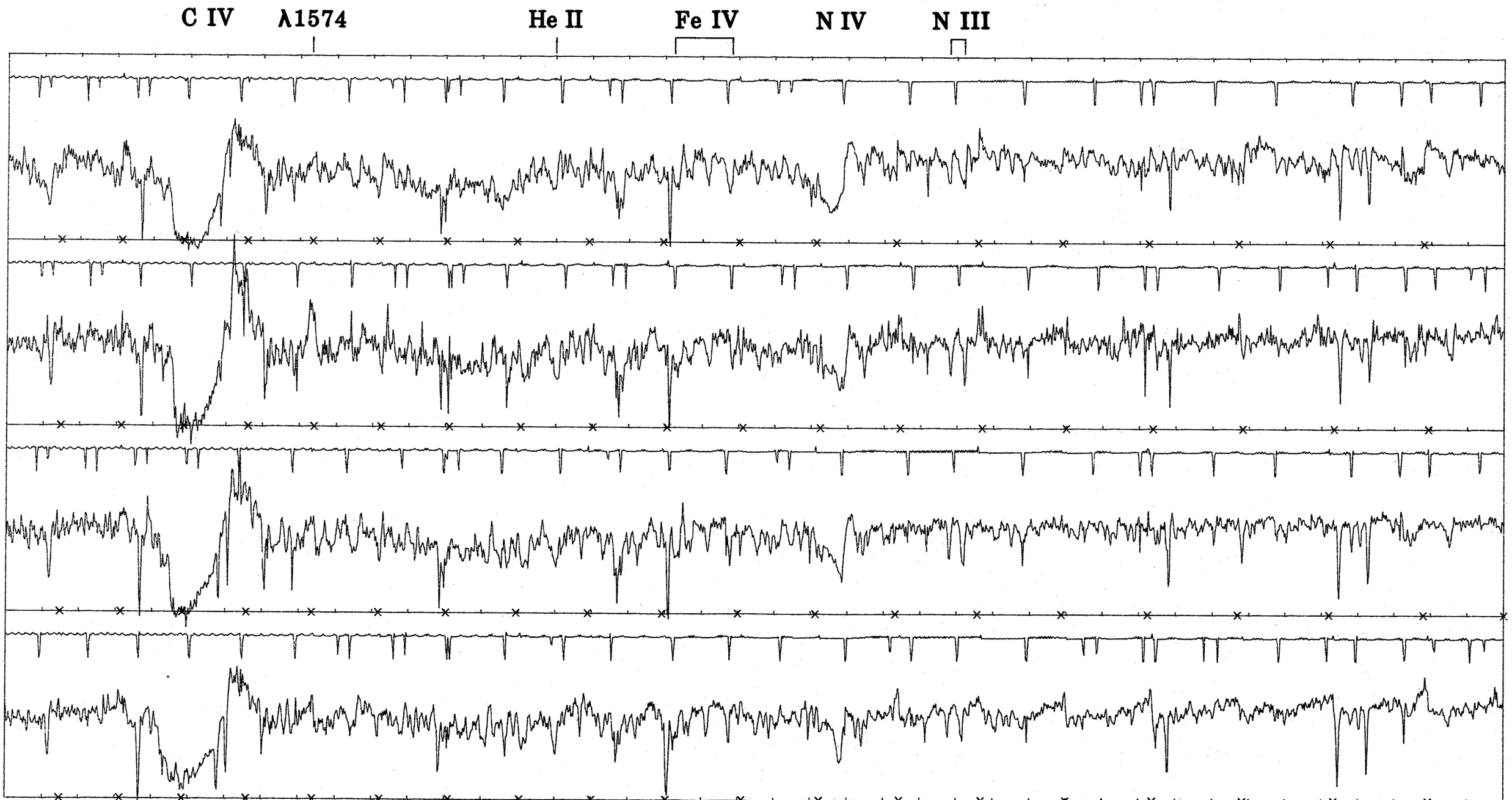
C IV
λ1574
He II
Fe IV
N IV
N III
1500
1520
1540
1560
1580
1600
1620
1640
1660
1680
1700
1720
1740
1760
1780
1800
1820
1840
1860
1880
1900

LUMINOSITY EFFECTS AT O9.5

The Si IV λλ1394,1403 doublet shows no stellar-wind effect in either the dwarf or the giant at this spectral type, but it develops gradually as a function of luminosity from classes II through Ia.

Since the N V λλ1239, 1243 and C IV λλ1548, 1551 stellar-wind effects in the lower luminosity spectra have declined by this spectral type, they now display a positive luminosity dependence as well.

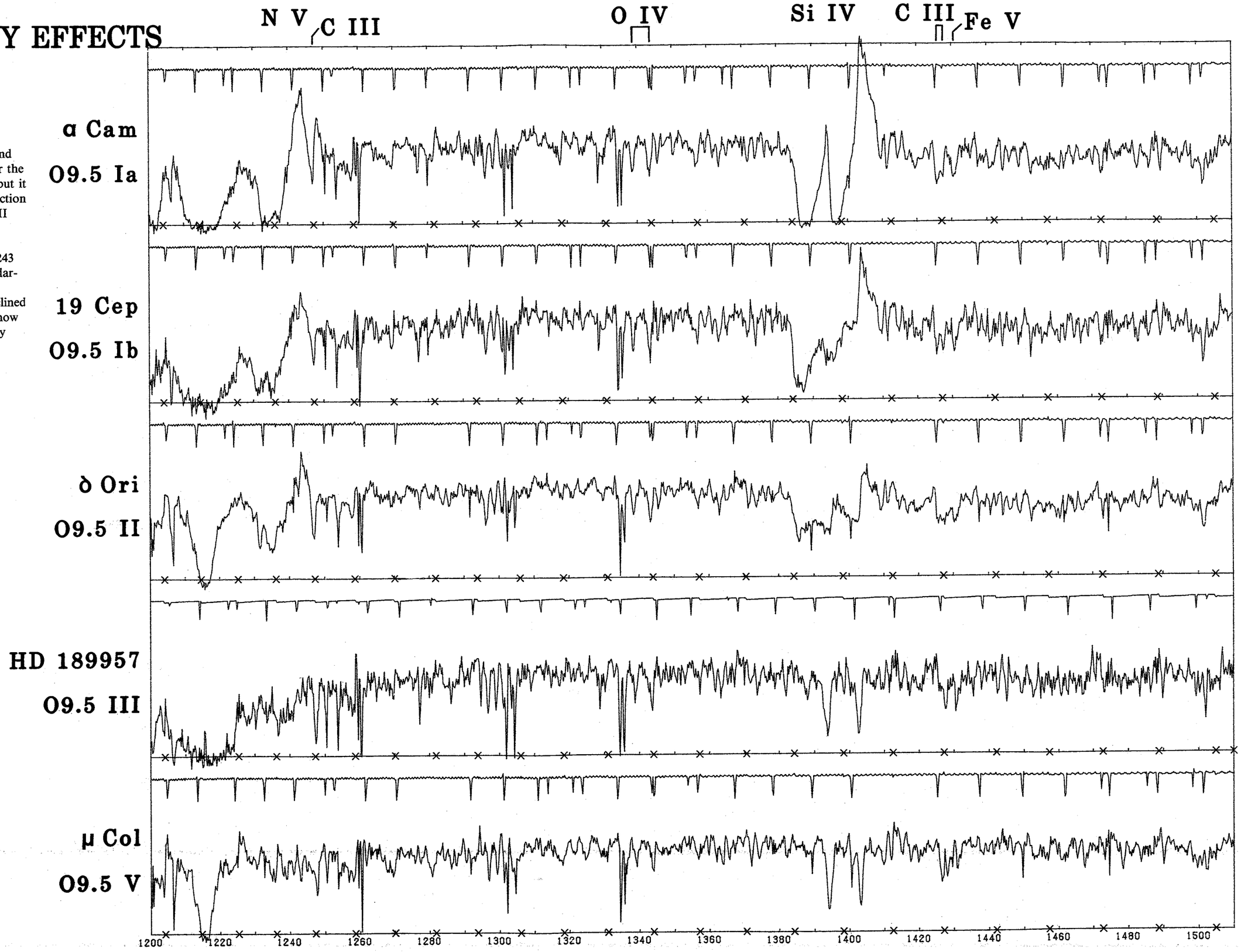

C IV He II Fe IV N IV N III

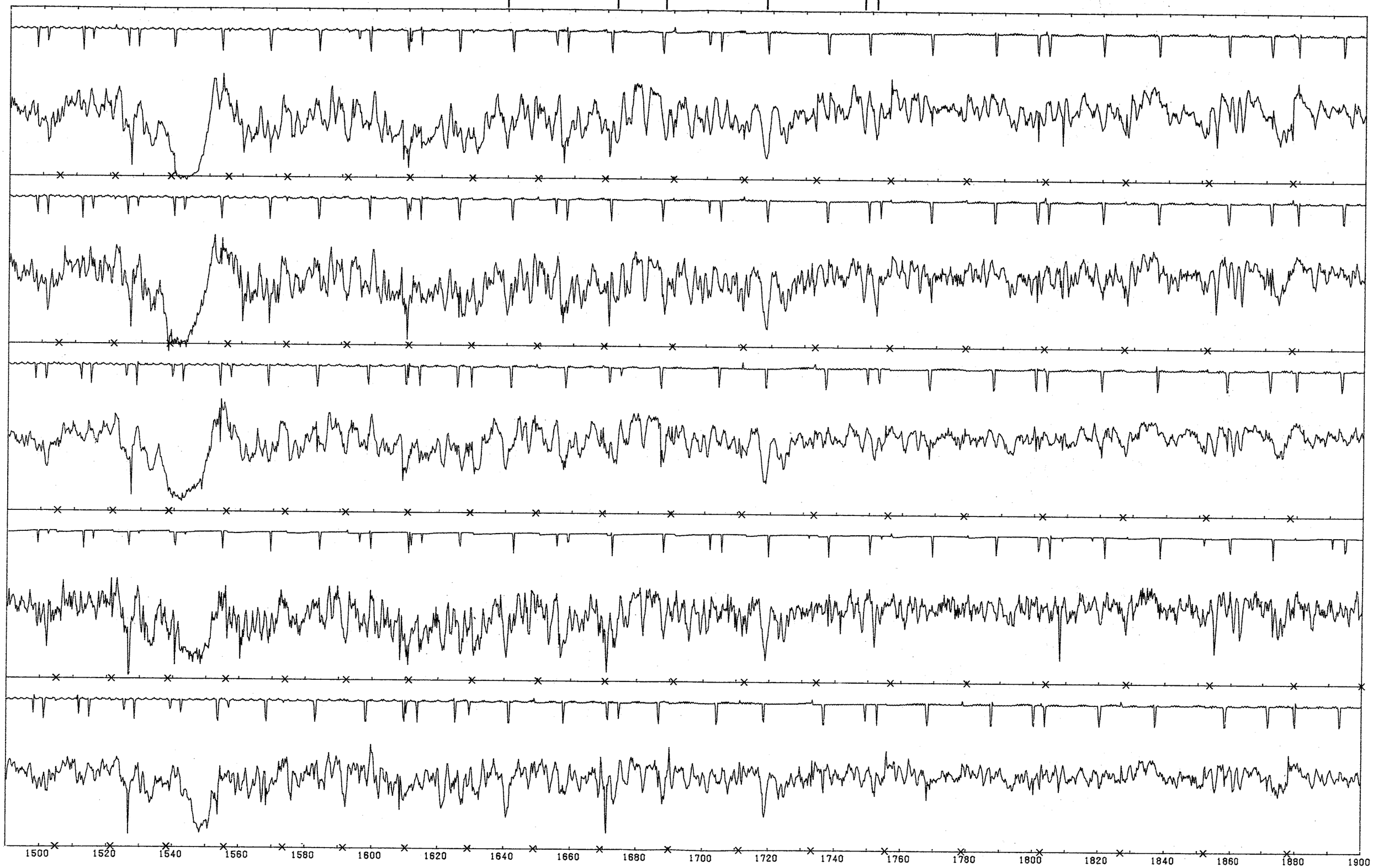

EARLY O DWARFS

This and the following two montages present samples within restricted spectral-type ranges, to demonstrate that the ultraviolet spectra of the primary optical standards are indeed representative, and that the ultraviolet spectra of normal O stars with the same optical types correspond in remarkable detail.

Note that Fe V λ1429 = λ1430 in the O3 and O4 spectra, but λ1429 < λ1430 at O5 and later. Again, note the marked increase in N III λ1748/λ1752 between O3 and O4, just as in the earlier comparison between the primary standards HDE 303308 and HD 46223.

An unusual feature in the spectrum of HD 93250 is the unsaturated C IV λλ1548, 1551 wind absorption, indicating either an otherwise unrecognized, later-type companion, or some other unidentified phenomenon.

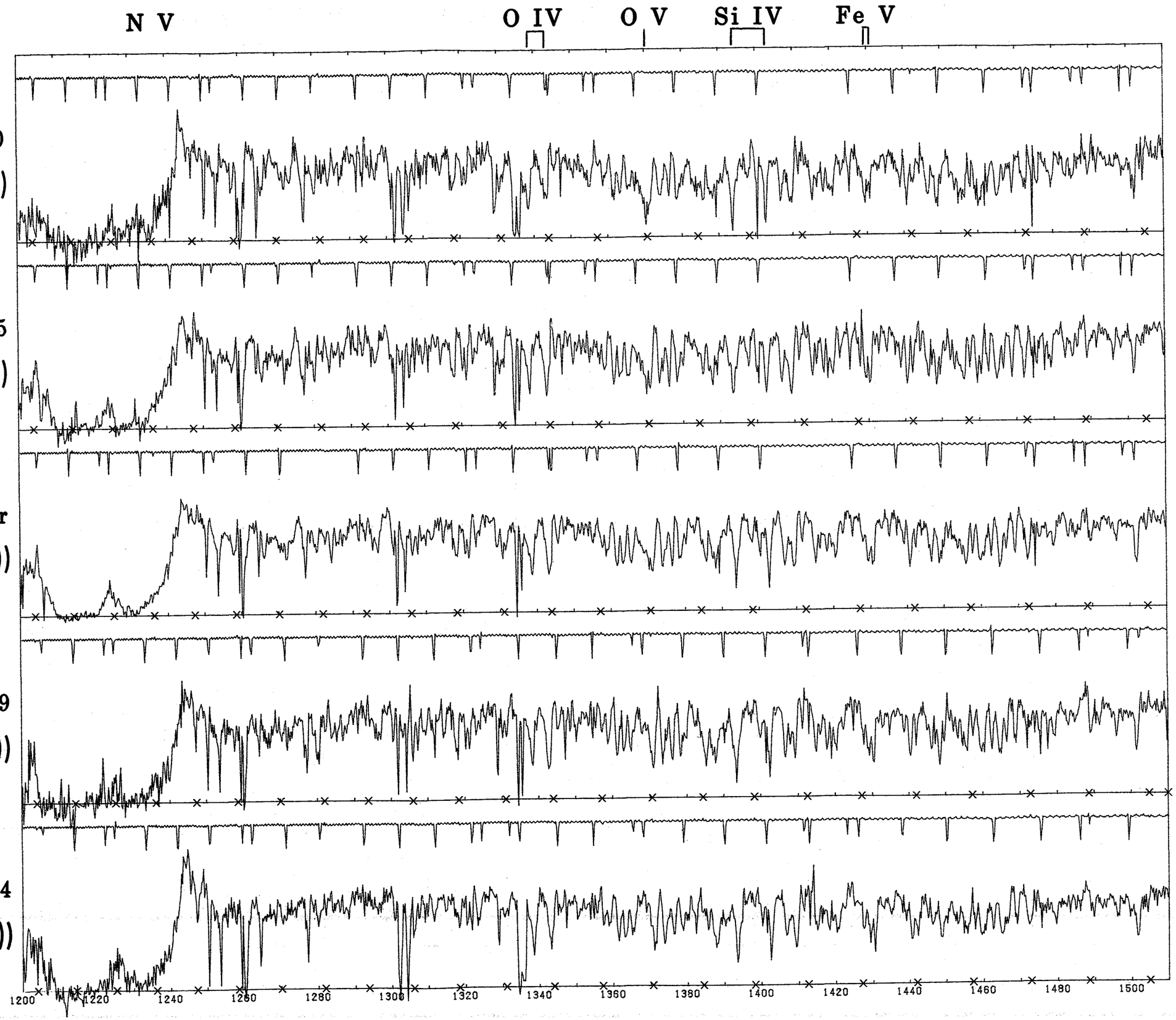

C IV He II N IV N III

1500 1520 1540 1560 1580 1600 1620 1640 1660 1680 1700 1720 1740 1760 1780 1800 1820 1840 1860 1880 1900

MIDDLE O DWARFS

The strong N V λλ1239, 1243 and C IV λλ1548, 1551 stellar-wind profiles decline rapidly from saturation in the O6.5 V-O7.5 V range.

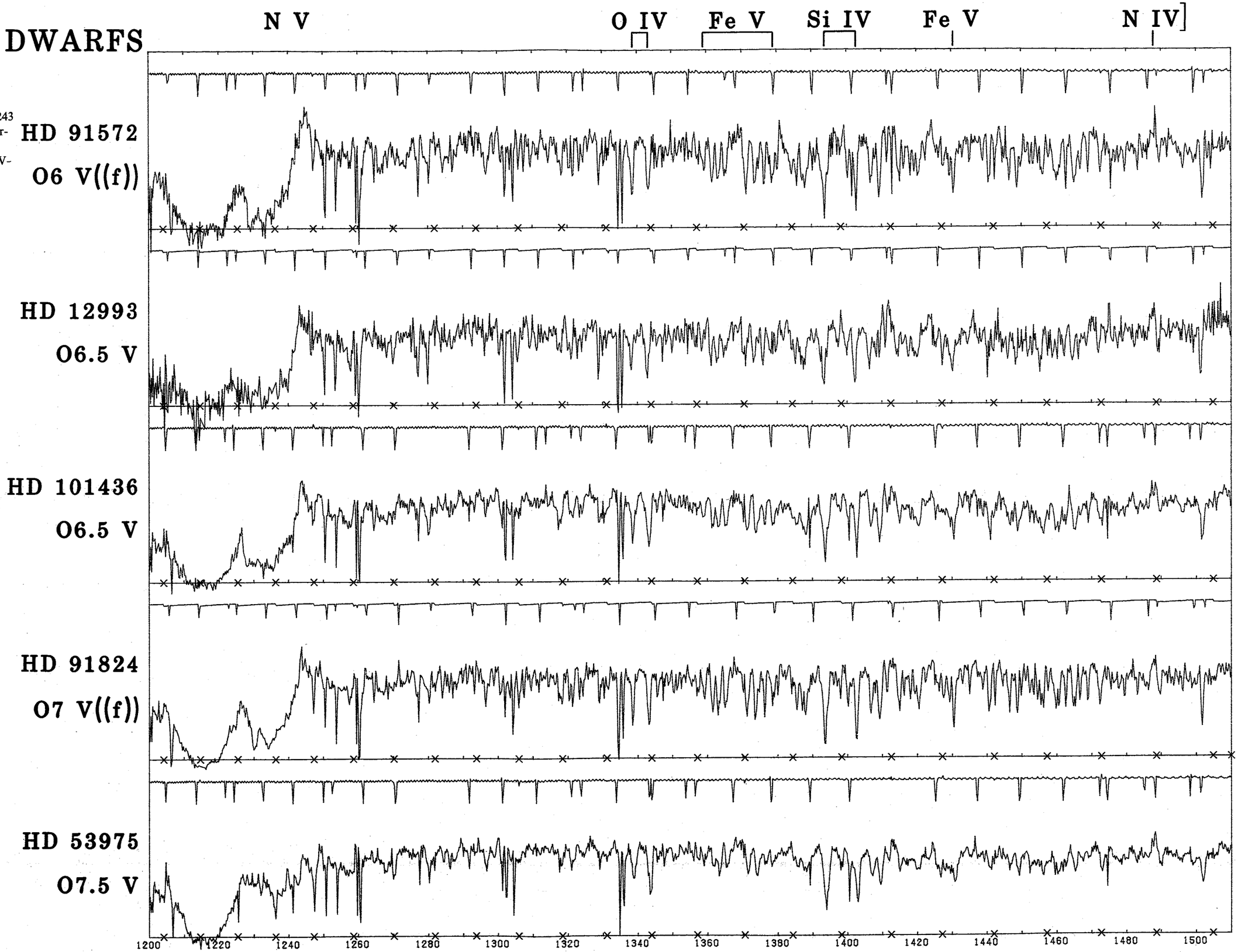

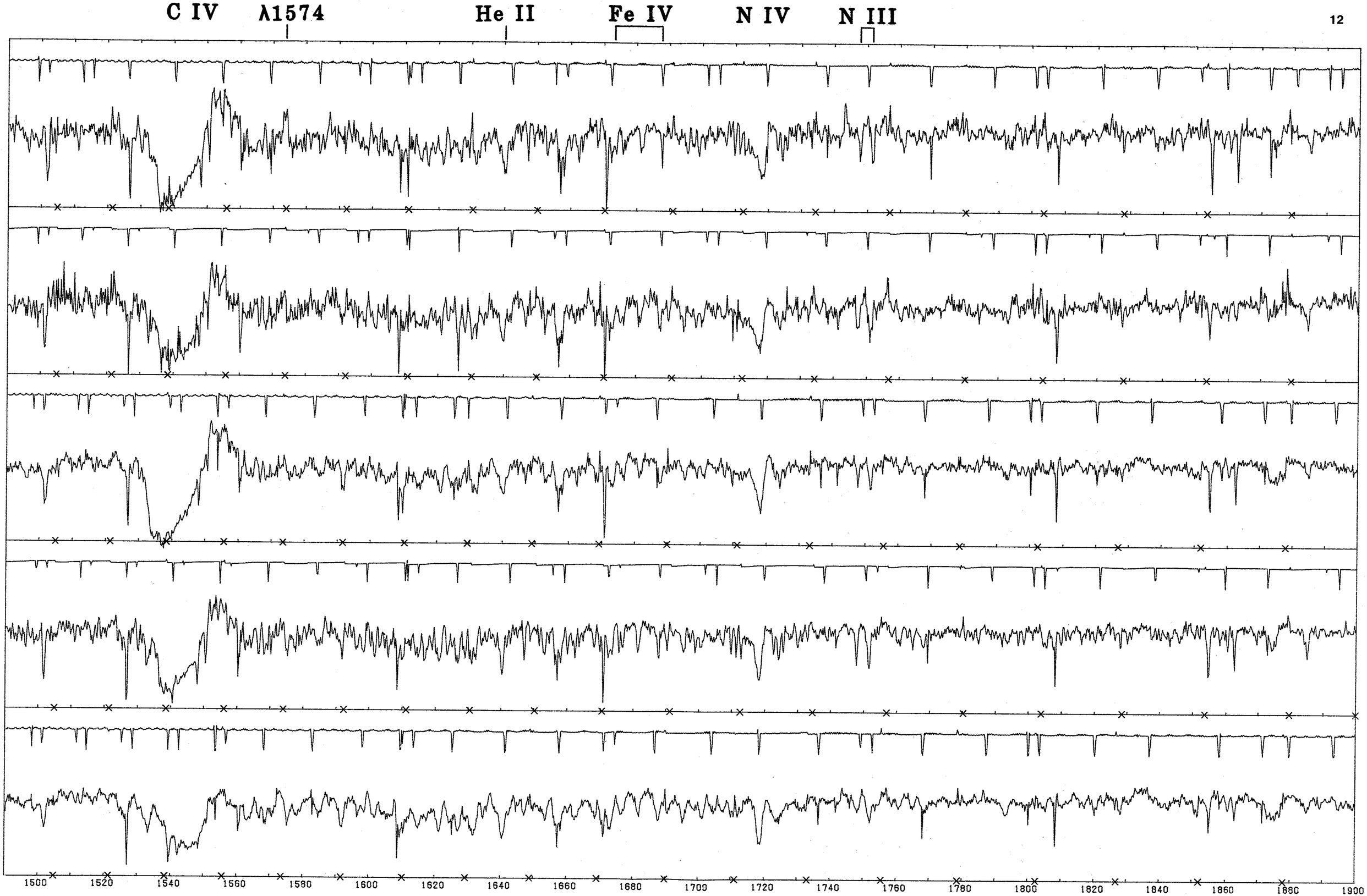
C IV
λ1574
He II
Fe IV
N IV
N III
1500
1520
1540
1560
1580
1600
1620
1640
1660
1680
1700
1720
1740
1760
1780
1800
1820
1840
1860
1880
1900

LATE O DWARFS

The N V λλ1239, 1243 wind profile disappears after O8 V, while C IV λλ1548, 1551 declines from a moderate P Cyg profile to a wind absorption trough alone through this spectral range.

C III λλ1426, 1428 strengthen relative to Fe V λ1430 in this range of spectral types.

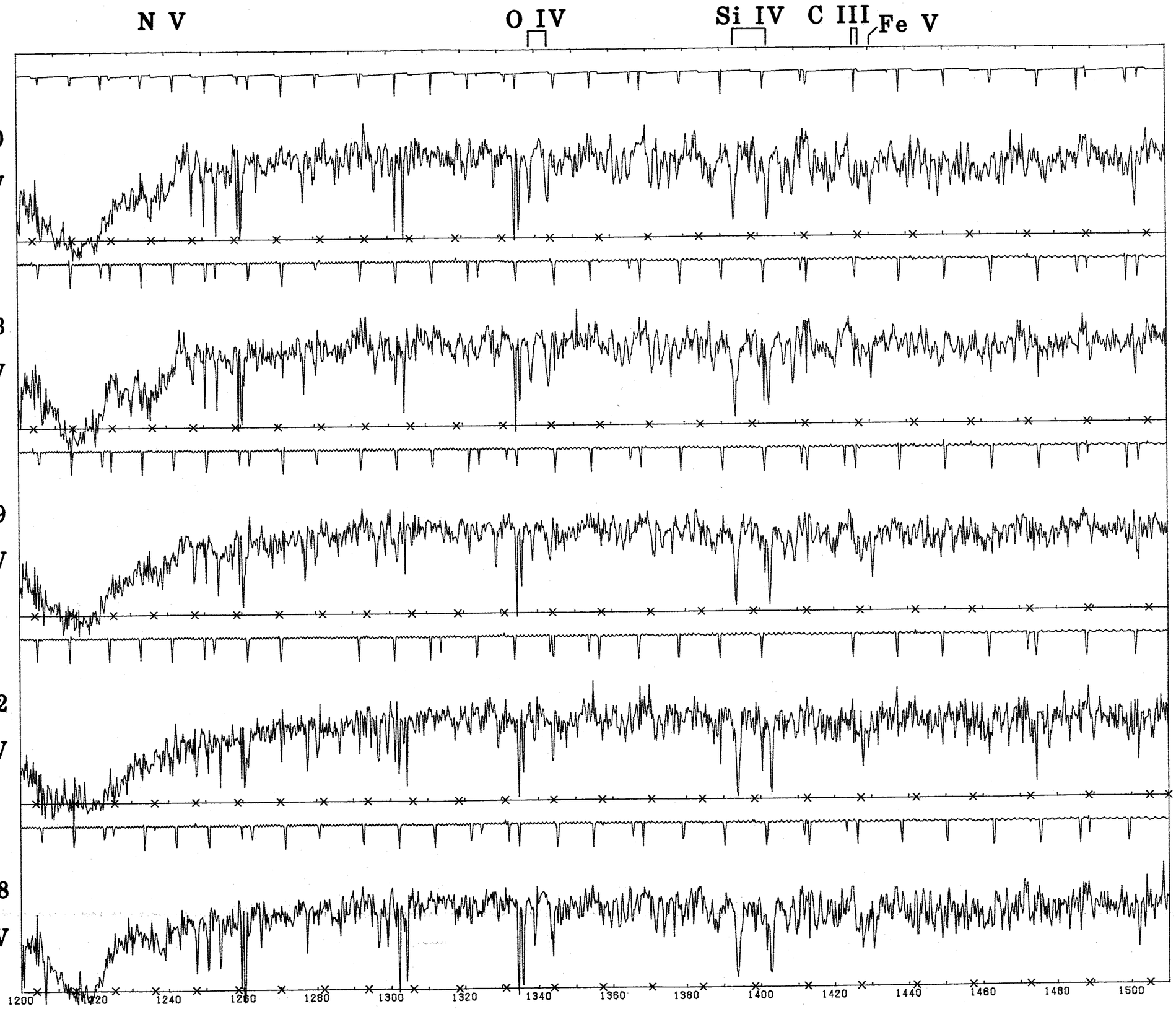

C IV He II N IV N III

1500 1520 1540 1560 1590 1600 1620 1640 1660 1680 1700 1720 1740 1760 1780 1800 1820 1840 1860 1880 1900

EARLY O GIANTS

HDE 269810 is in the Large Magellanic Cloud (references 7, 10). Note the distinctive O V λ1371 stellar-wind profile, characteristic of O3 giant and supergiant spectra.

Si IV λλ1394, 1403 shows weak or no wind effects in the O3 III and O5 III spectra, due to the high ionization. In the normal O6 III and later giant spectra, however, the Si IV develops a well marked shortward absorption trough.

ξ Per represents a small percentage of O giants with an enhanced Si IV stellar-wind feature. This effect may be related to the rapid rotation or to some other peculiarity; alternatively, it may imply a somewhat higher luminosity than indicated by the optical criteria. The Si IV profile in ξ Per would be appropriate for luminosity class II.

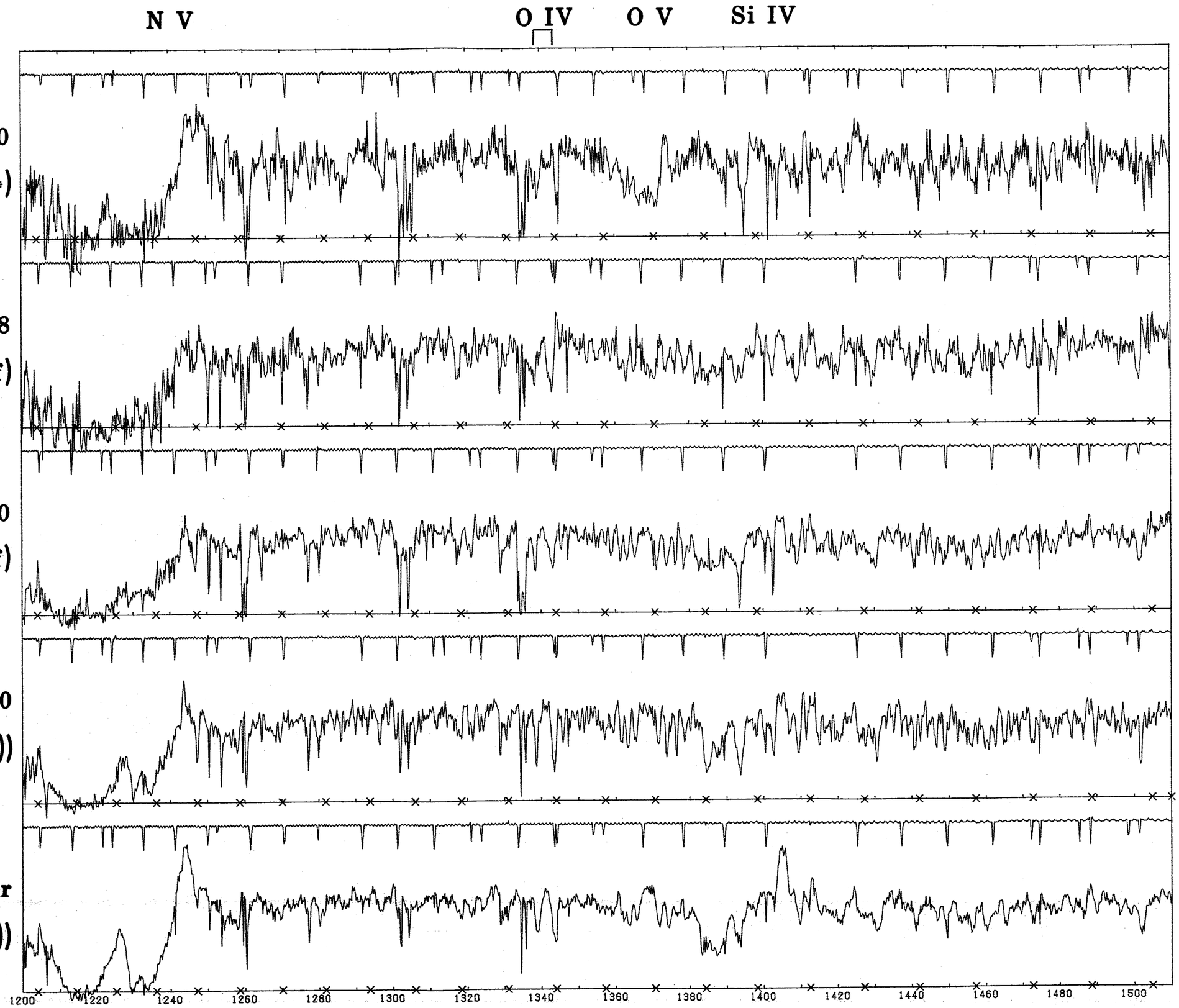

C IV He II N IV N III

1500 1520 1540 1560 1580 1600 1620 1640 1660 1680 1700 1720 1740 1760 1780 1800 1820 1840 1860 1880 1900

LATE O GIANTS

All of these spectra display the pronounced Si IV λλ1394, 1403 shortward wind absorption troughs which are typical of normal giants.

Blue-violet spectrograms of λ Ori and HD 48434 are reproduced in reference 3, and yellow-red ones of λ Ori and ι Ori in reference 8.

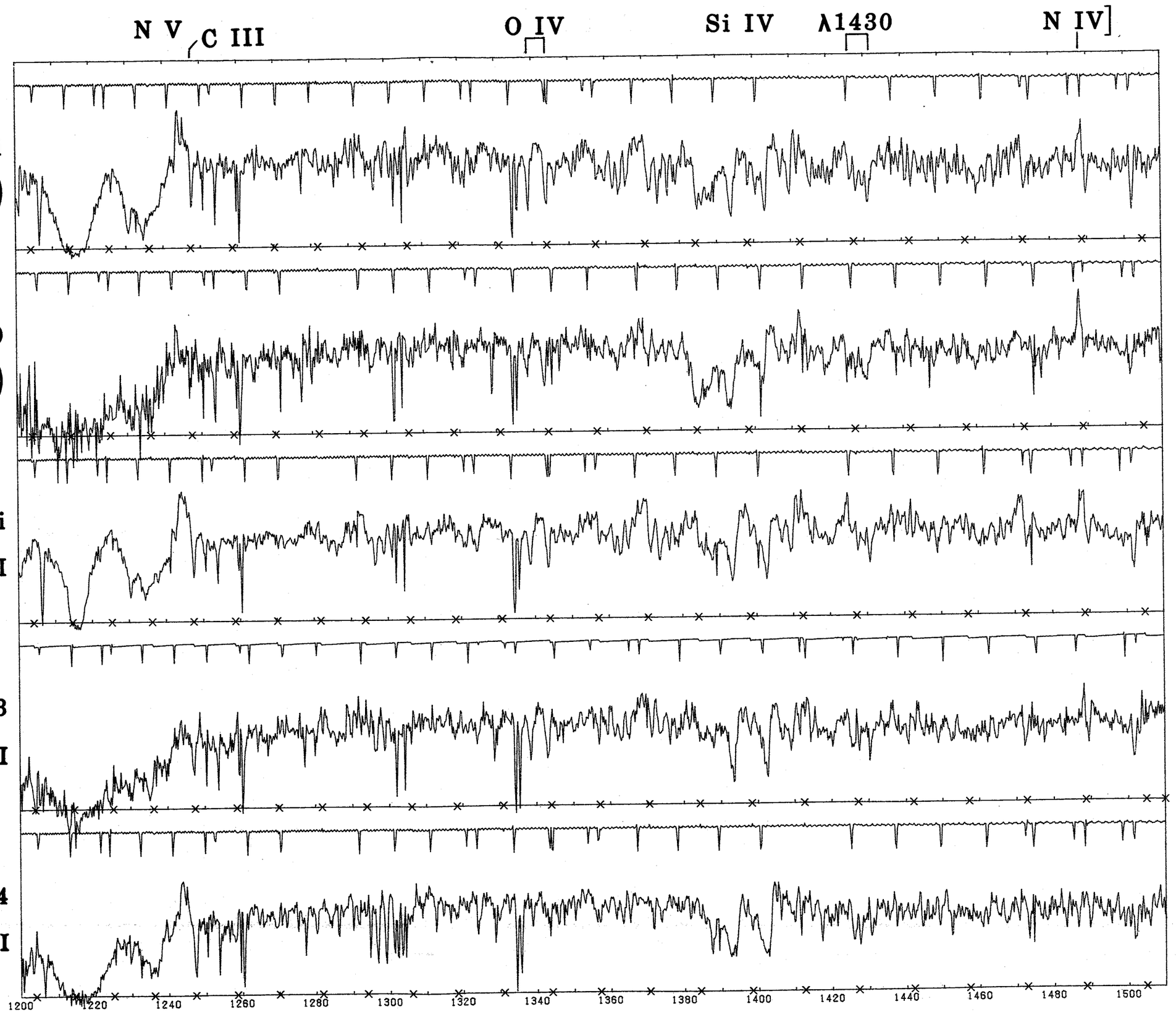

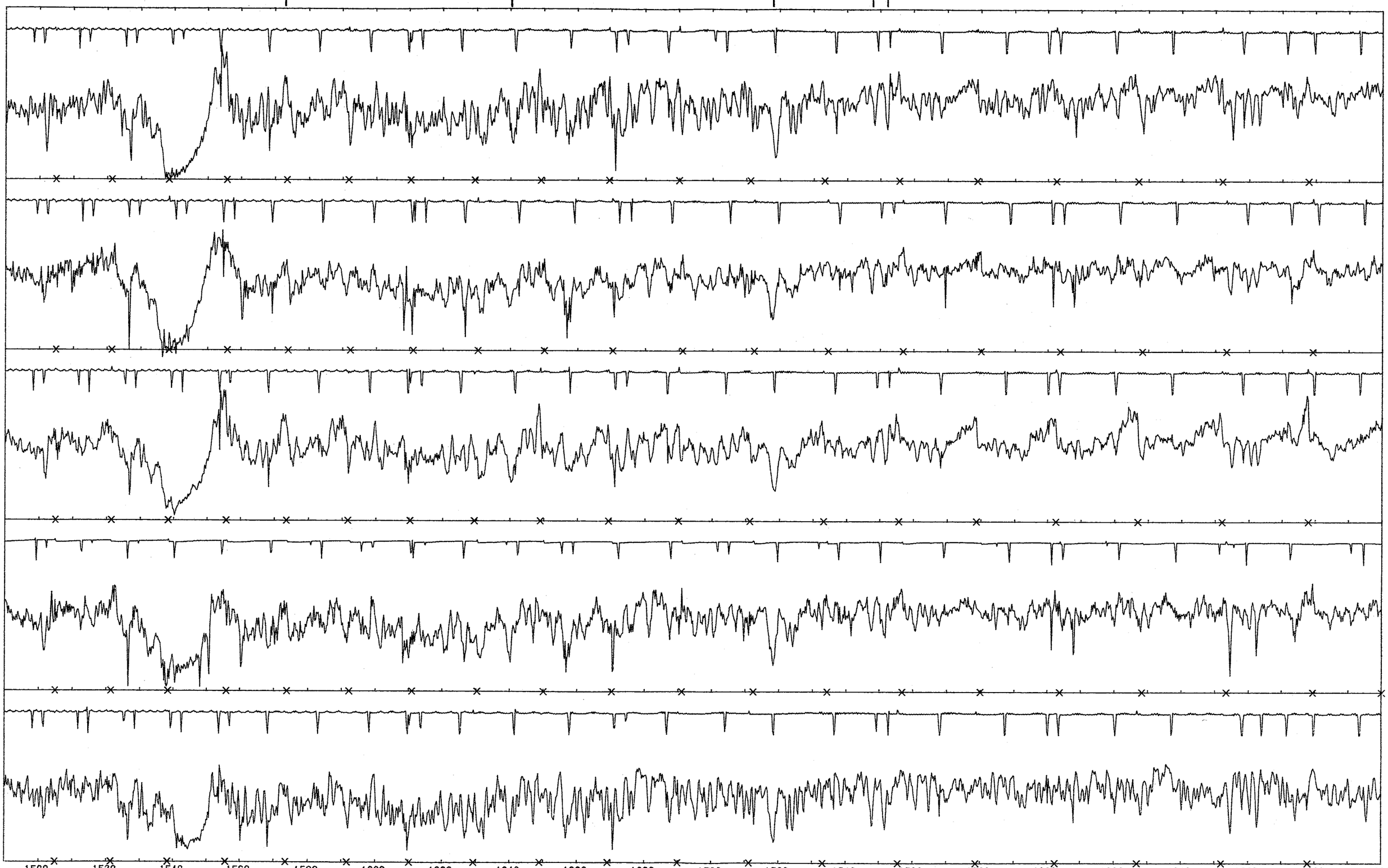
C IV λ1574
He II
N IV
N III
1500
1520
1540
1560
1580
1600
1620
1640
1660
1680
1700
1720
1740
1760
1780
1800
1820
1840
1860
1880
1900

BRIGHT GIANTS

The luminosity class II spectra have Si IV λλ1394, 1403 stellar-wind profiles which are intermediate between those of classes III and Ib at a given spectral type. Type O8 apparently corresponds to the Si IV temperature maximum at this luminosity class.

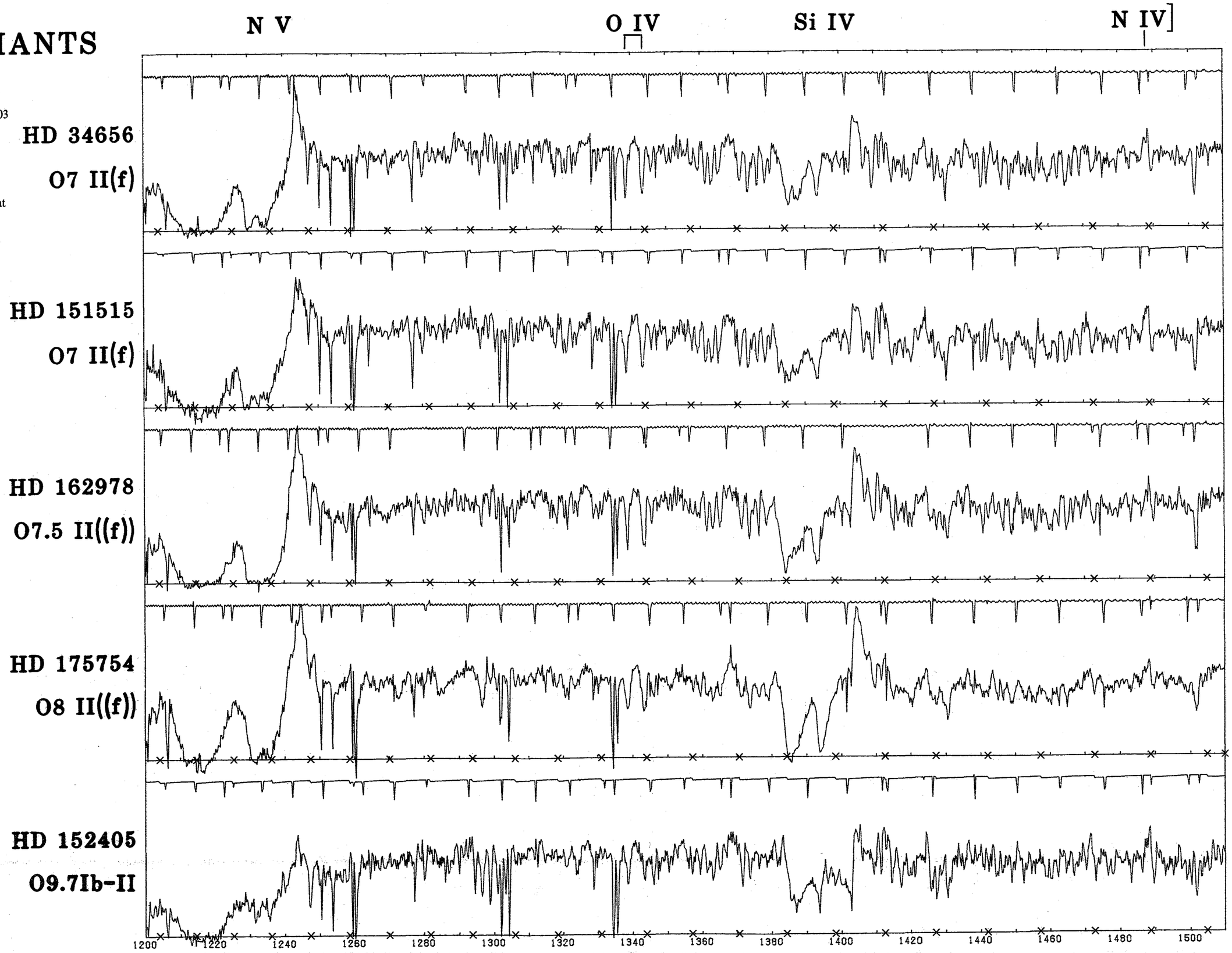

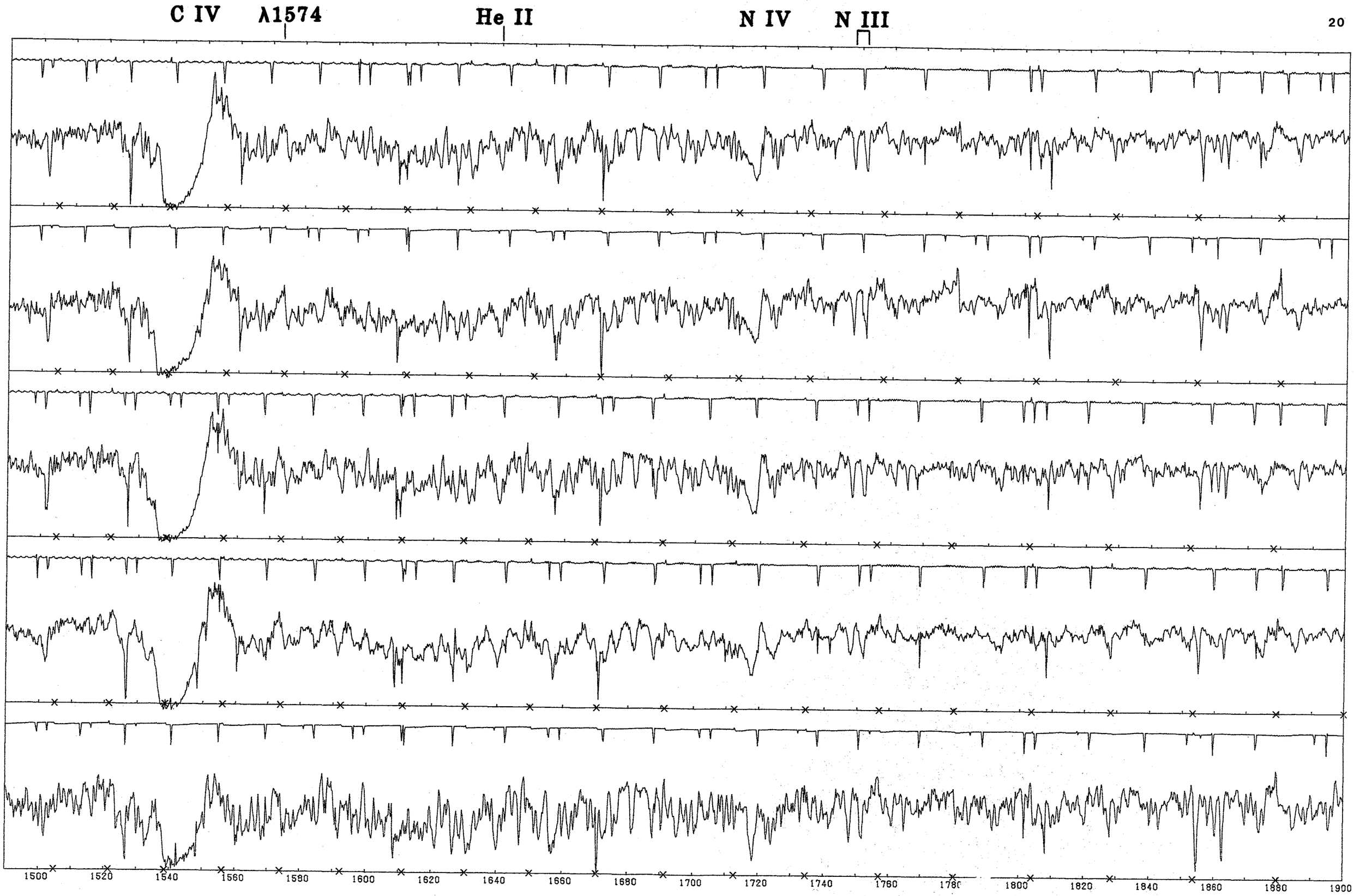
C IV λ1574
He II
N IV
N III
1500
1520
1540
1560
1580
1600
1620
1640
1660
1680
1700
1720
1740
1760
1780
1800
1820
1840
1860
1880
1900

Ib SUPERGIANTS

Note the change in appearance of the λ1430 region in passing from the O7 spectra to those of later types, due to the strengthening of C III λλ1426, 1428 relative to Fe V λ1430. N IV λ1718 exhibits a progressive decline in the stellar-wind effect through this spectral-type range.

A blue-violet spectrogram of HD 192639 is reproduced in reference 4. ζ Ori is moderately nitrogen-deficient (reference 6).

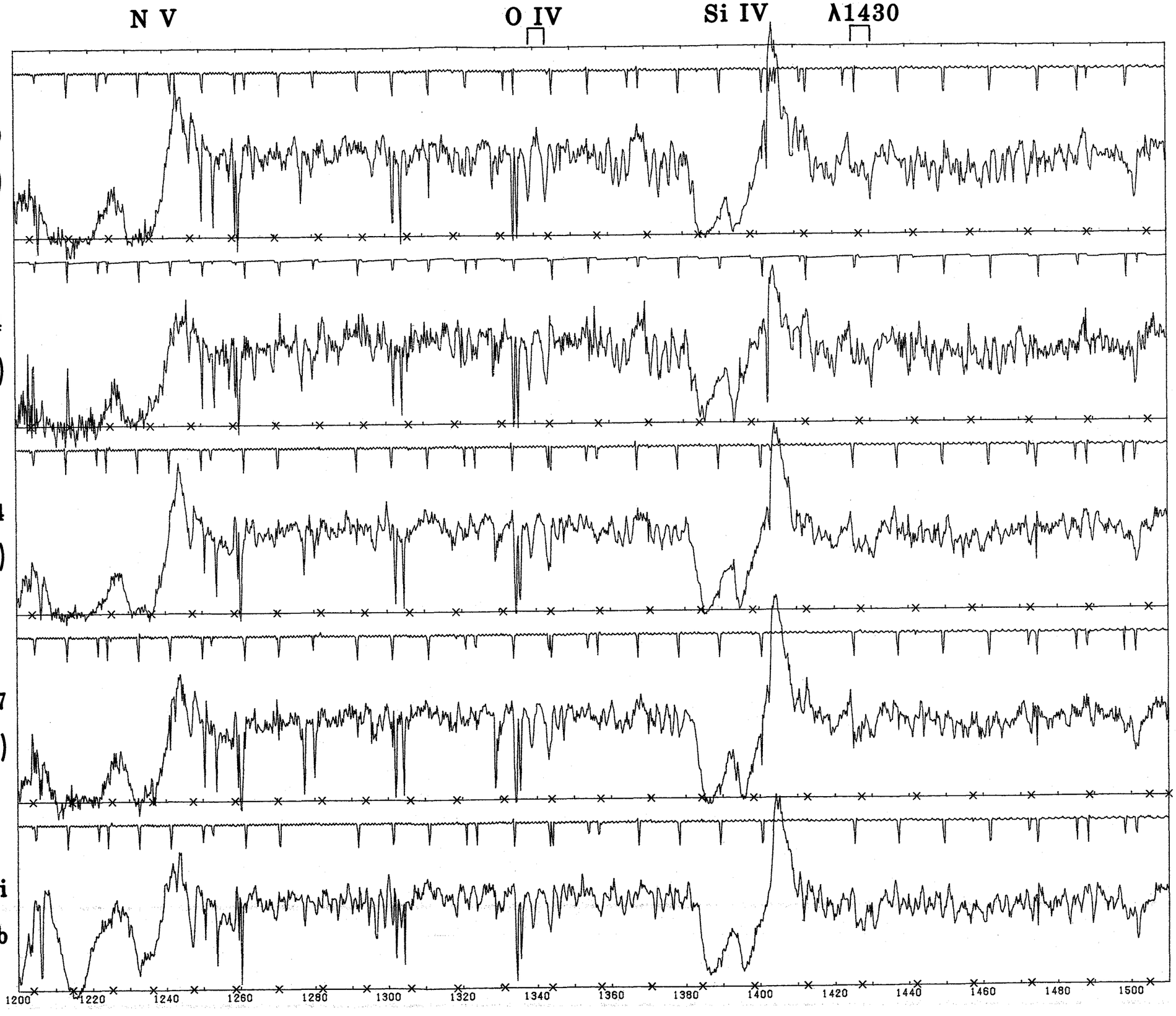

C IV He II N IV N III

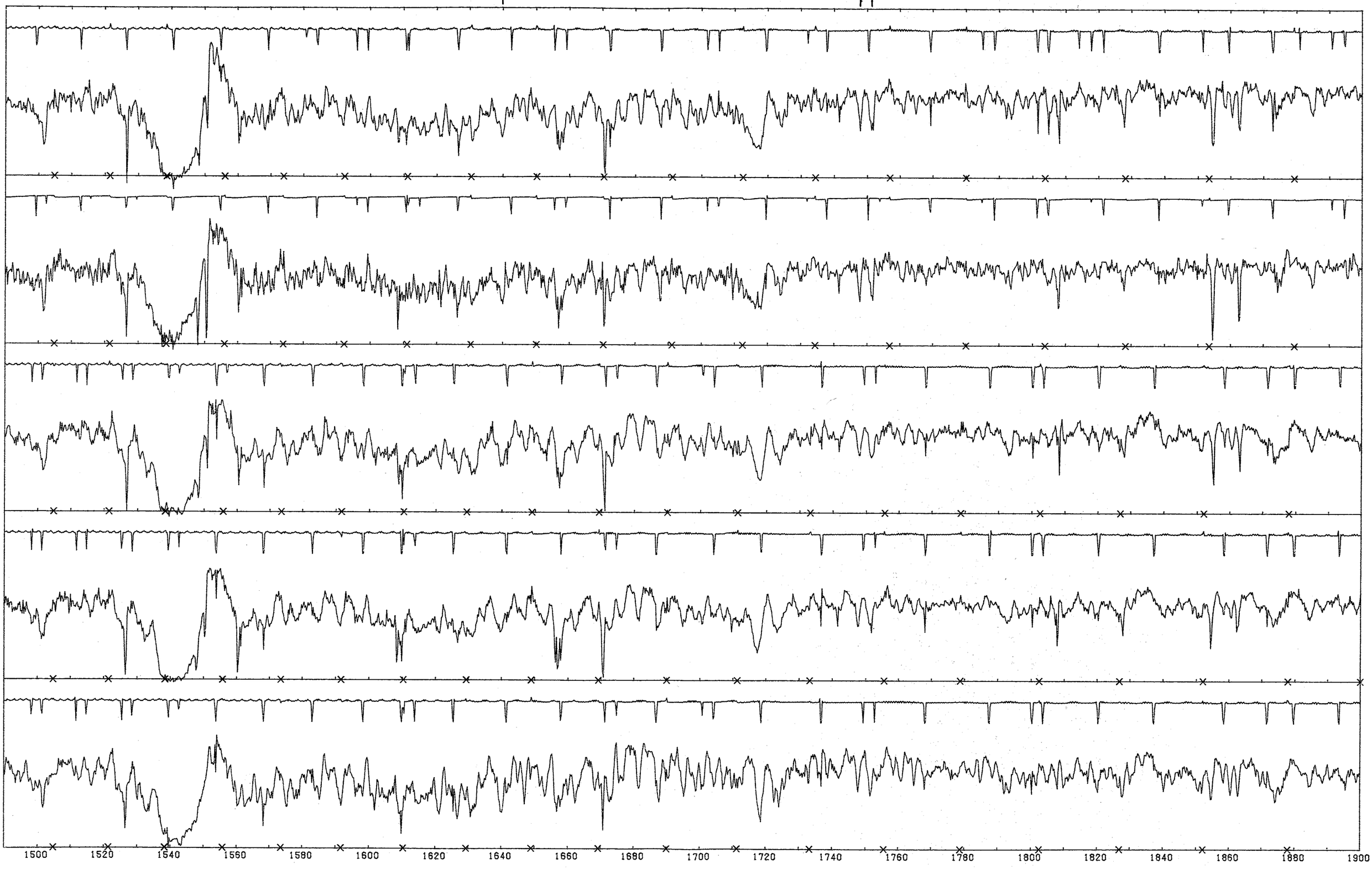

EARLY Of SUPERGIANTS

All of the O4 If spectra have similar, intermediate Si IV λλ1394,1403 stellar-wind profiles, due to their high ionization. The O3 If has an even weaker Si IV wind feature, as well as a distinctive O V λ1371 wind profile and weak N III λλ1748,1752, demonstrating higher ionization than the O4 If's, as was first found optically (reference 2). The strong correspondence between photospheric and wind conditions is evident.

The O3-O5 If spectra all display a pronounced He II λ1640 wind feature, which disappears at later types.

HDE 269698 is in the Large Magellanic Cloud (reference 7). The spectrogram shown is an average of two observations (SWP 6967 and 8011).

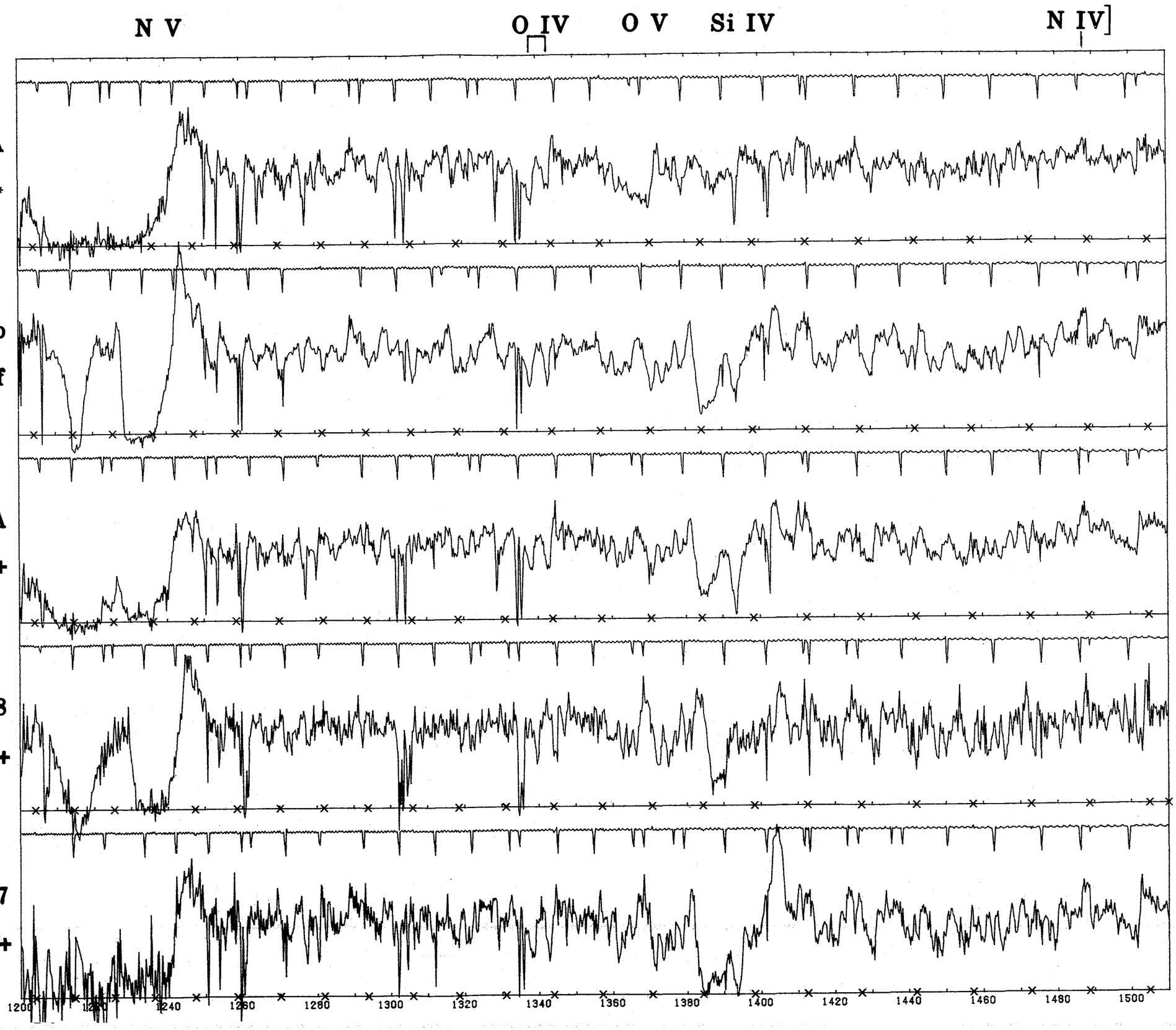

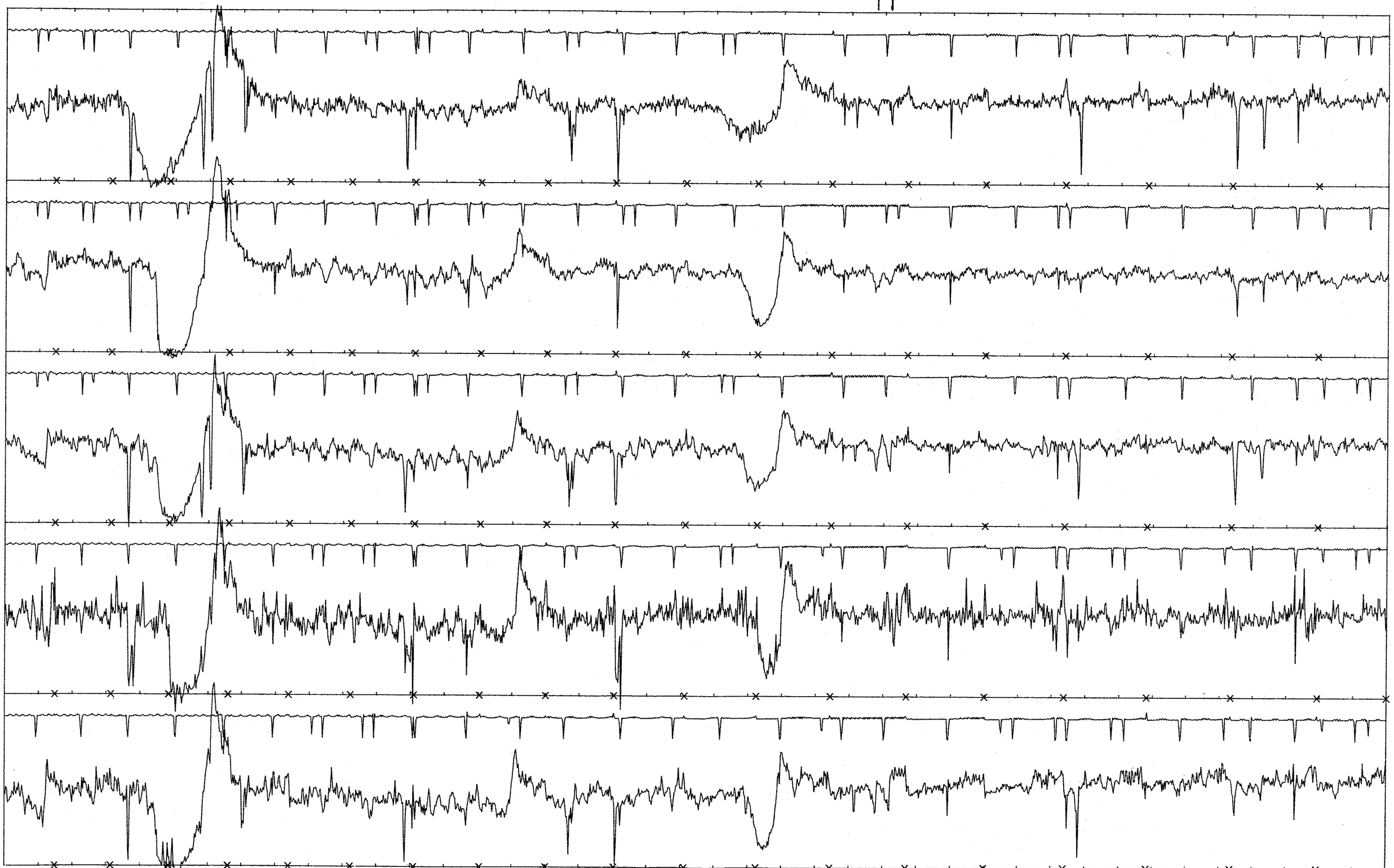
C IV
He II
N IV
N III
1500
1520
1540
1560
1580
1600
1620
1640
1660
1680
1700
1720
1740
1760
1780
1800
1820
1840
1860
1880
1900

MIDDLE Of SUPERGIANTS

All Of supergiants later than O4 have saturated Si IV λλ1394, 1403 stellar-wind profiles, in addition to N V λλ1239,1243 and C IV λλ1548,1551. In O3-O4 If spectra, the C IV wind profiles are stronger than the Si IV; at O5-O6 If, the two profiles have similar intensities; and at O6.5-O8.5 If the Si IV is stronger than the C IV. Again, the detailed correspondence between the ultraviolet wind features and the optical spectral types is remarkable.

Blue-violet spectrograms of λ Cep and HD 163758 are reproduced in reference 4, and of HD 151804 in reference 11, while yellow-red spectrograms of 9 Sge, HD 151804, and HD 112244 are shown in reference 8.

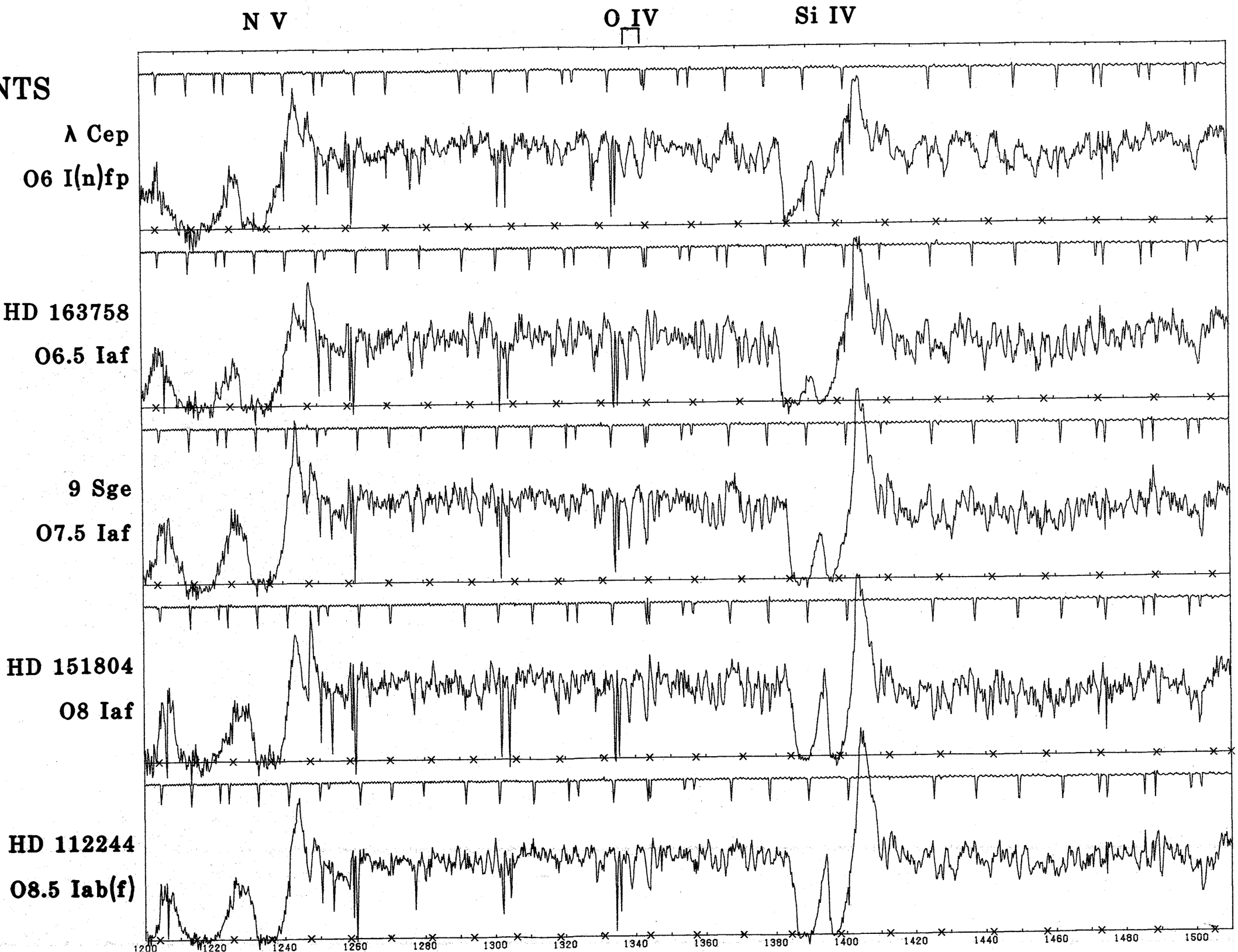

C IV He II N IV N III

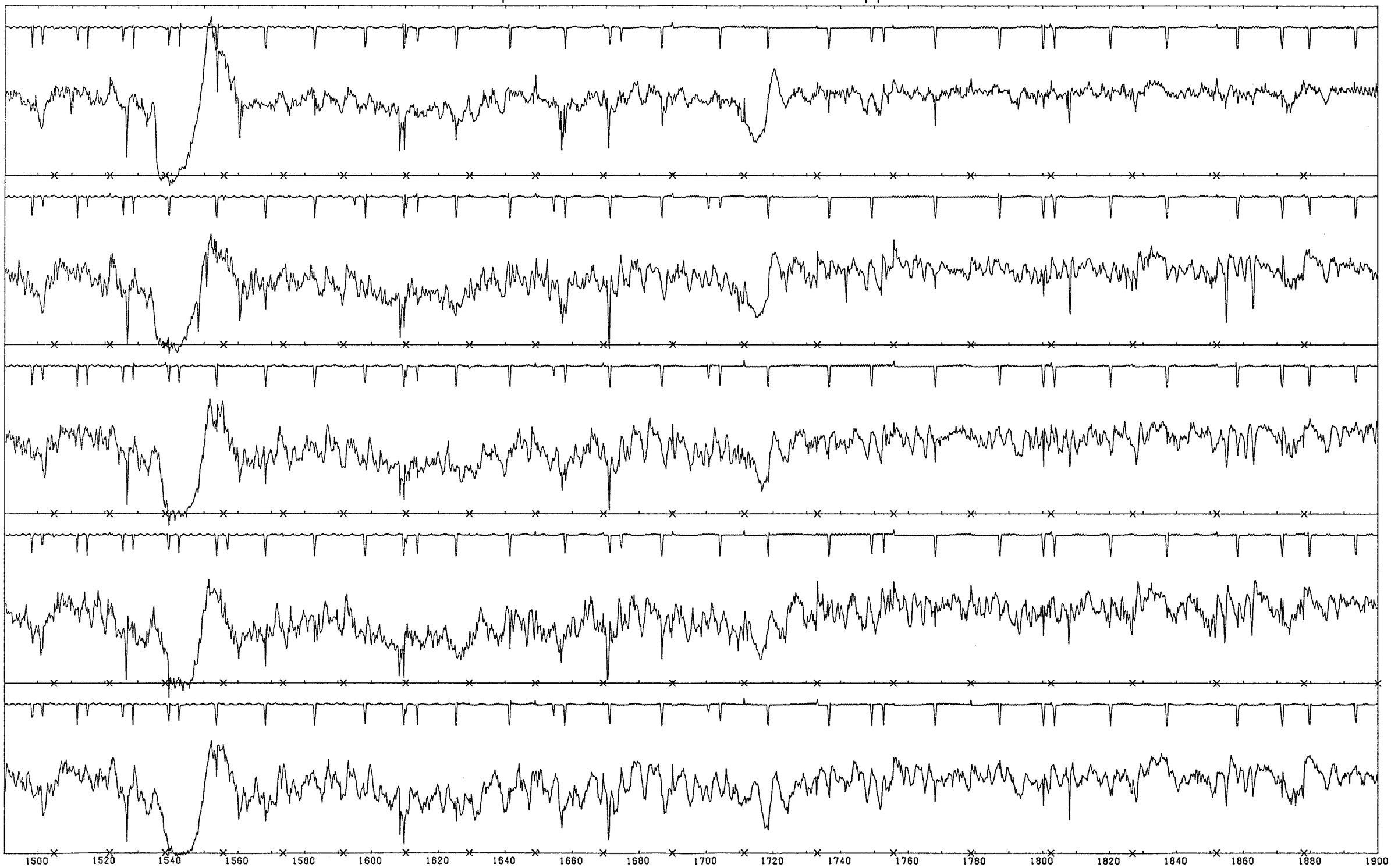

Iab SUPERGIANTS

The luminosity class Iab (and Ib) spectra have Si IV λλ1394, 1403 wind profiles which are intermediate between those of classes II and Ia, and are distinctly less saturated than the latter.

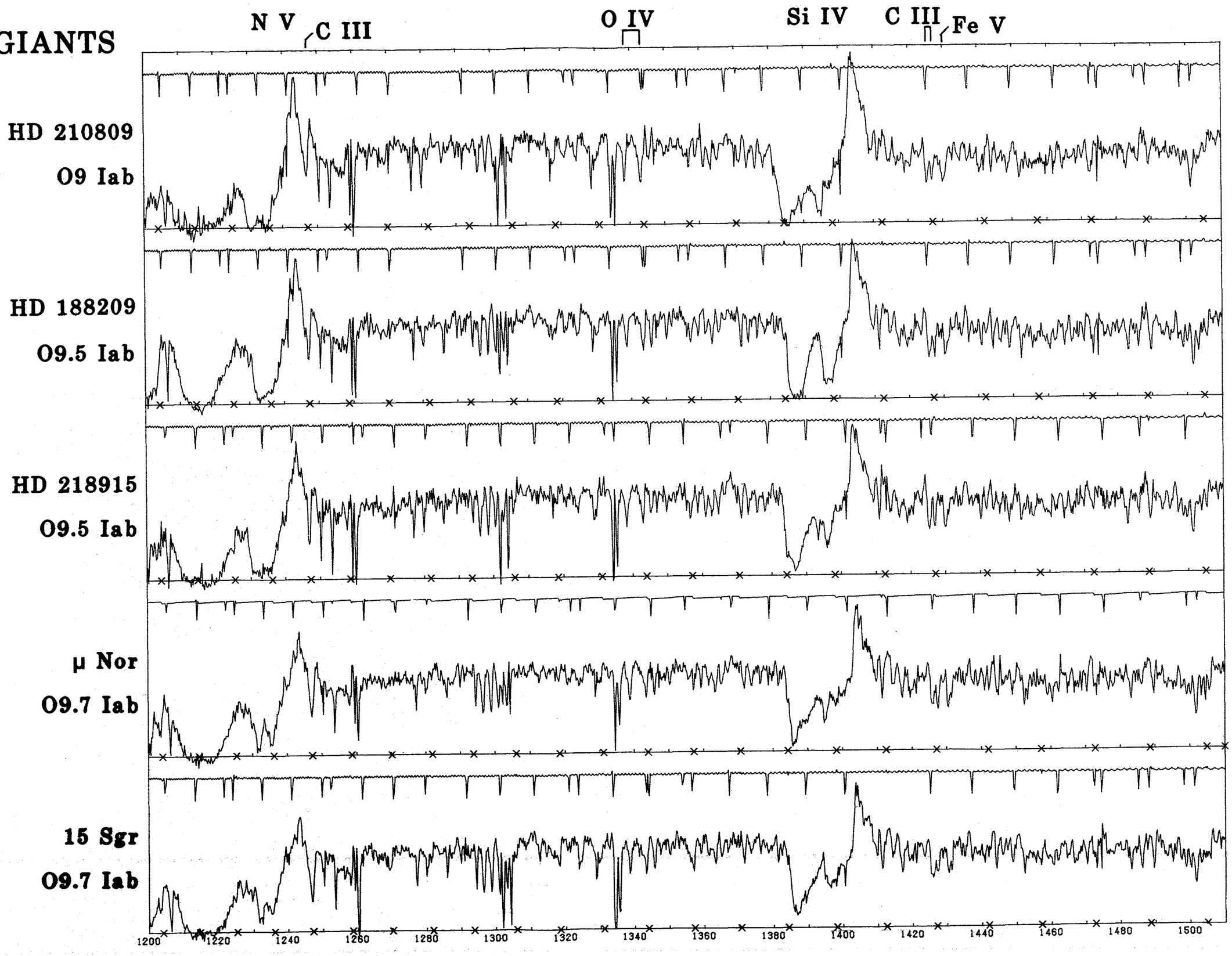

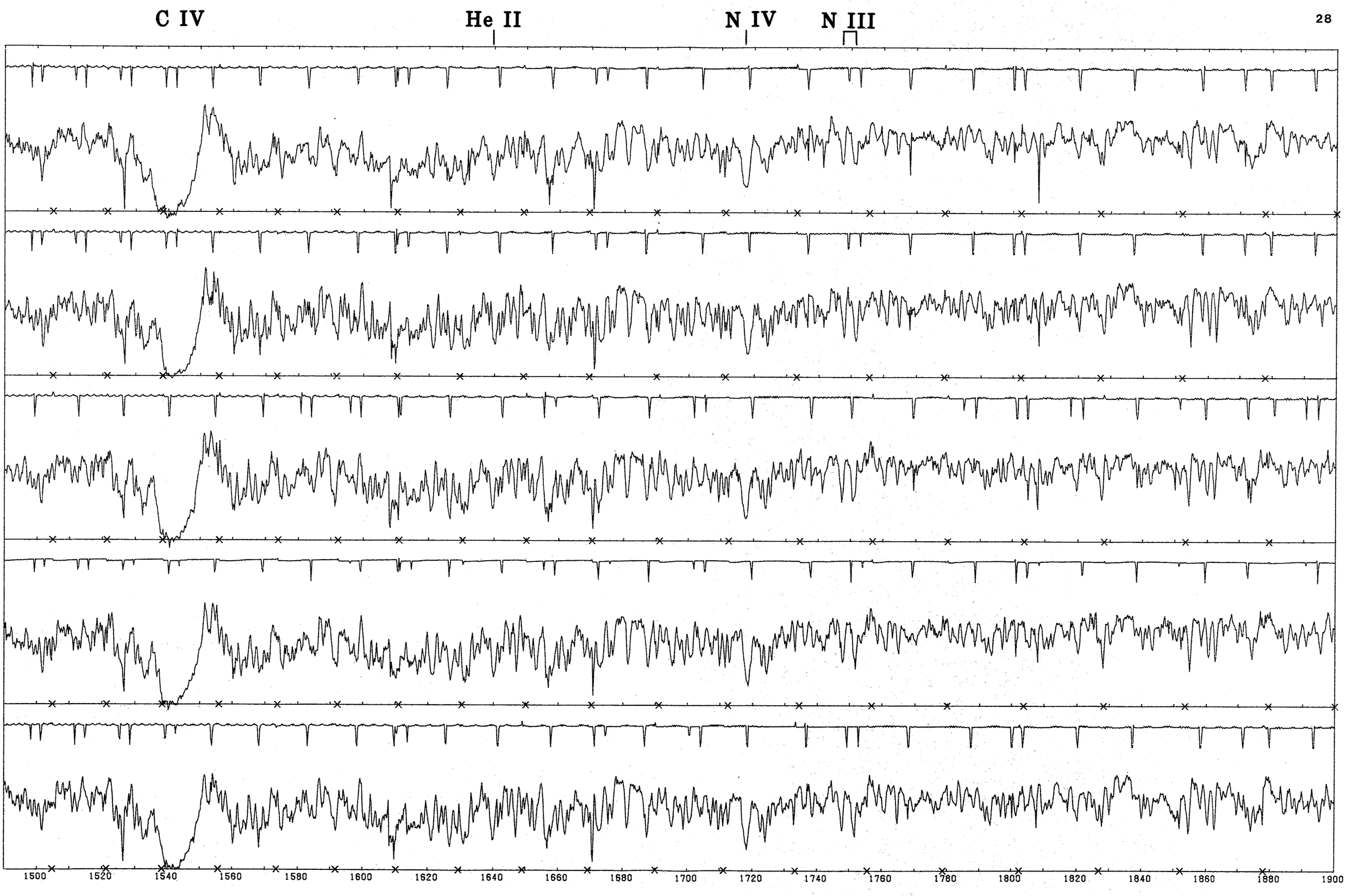
C IV
He II
N IV
N III
1500
1520
1540
1560
1580
1600
1620
1640
1660
1680
1700
1720
1740
1760
1780
1800
1820
1840
1860
1880
1900

Ia SUPERGIANTS

The Si IV λλ1394, 1403 stellar-wind profiles begin to show the effects of declining ionization at type B0 Ia.

HD 149404 is moderately carbon-deficient, while ε Ori is moderately nitrogen-deficient (reference 6).

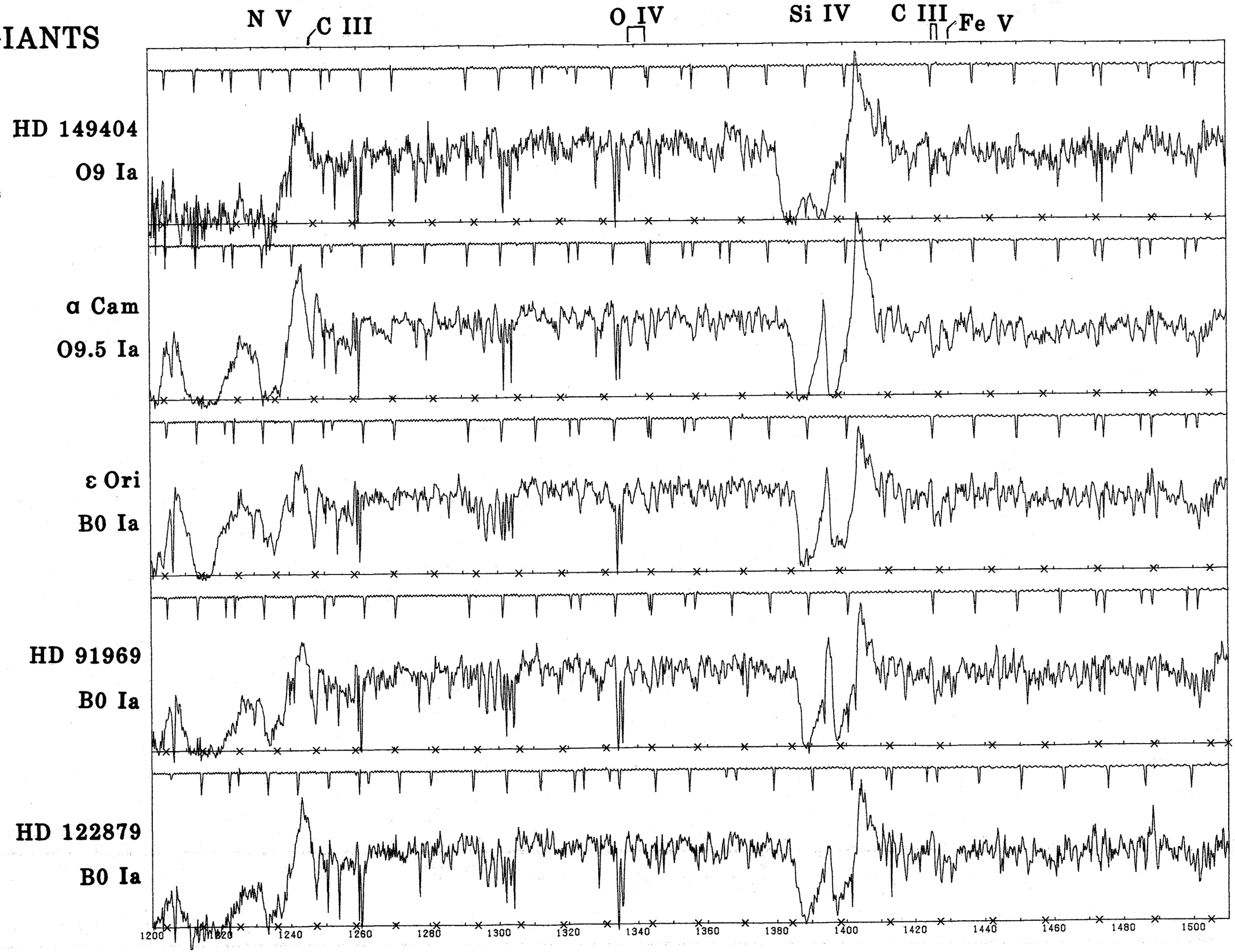

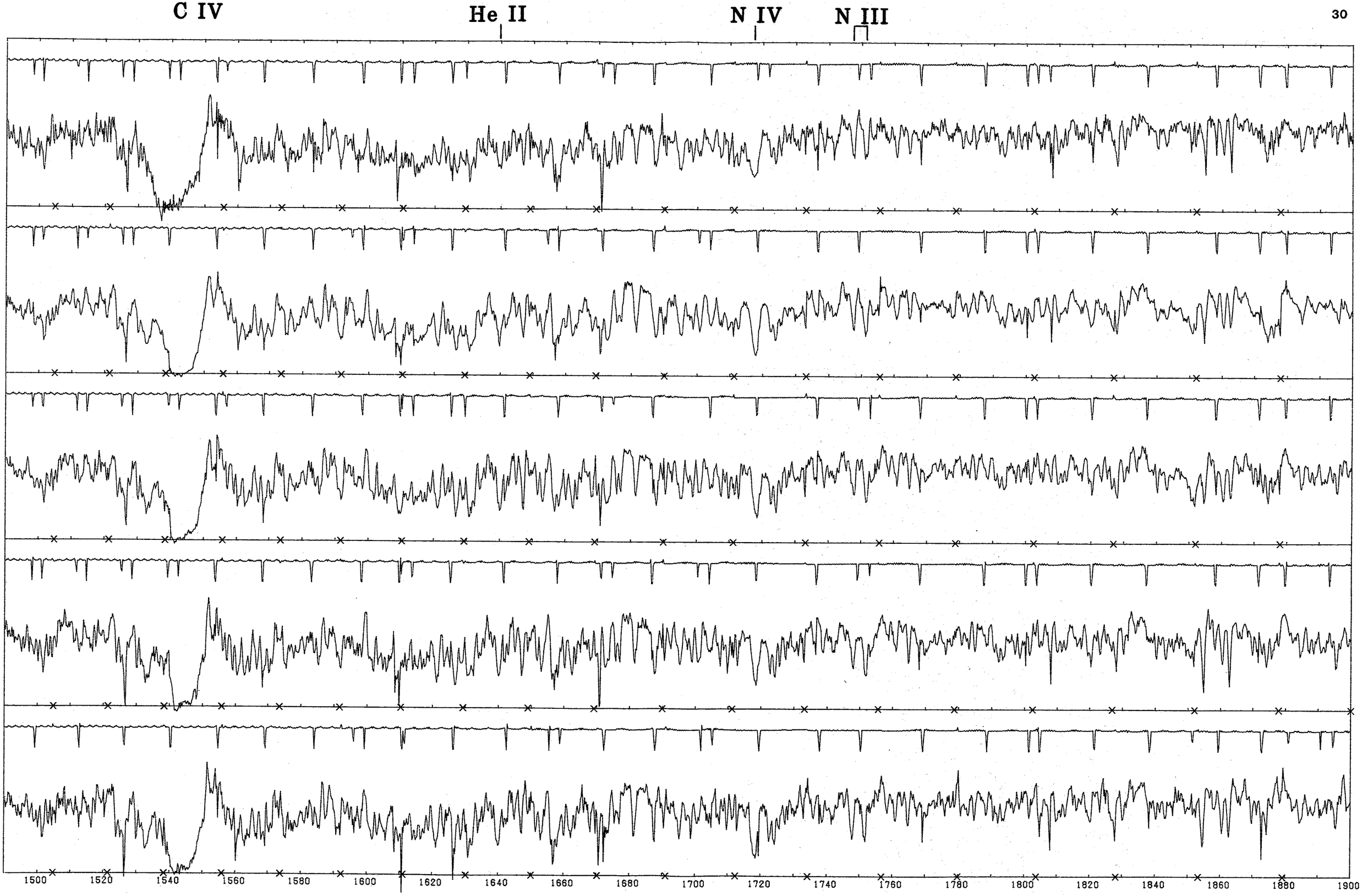
C IV
He II
N IV
N III
1500
1520
1540
1560
1580
1600
1620
1640
1660
1680
1700
1720
1740
1760
1780
1800
1820
1840
1860
1880
1900

WEAK WINDS

These O dwarfs have relatively weak stellar-wind features for their spectral types. Θ^1 Orionis C (Orion Nebula) and HD 5005A (NGC 281) are located in Trapezium systems, while HD 42088 excites the dusty H II region NGC 2175. These stars may be nearer to the zero-age main sequence than the typical O dwarfs.

In addition, the wind features in the spectrum of Θ^1 Ori C, especially the shortward absorption of C IV λλ1548, 1551, are strongly variable. Further investigation is required to determine whether these recurrent variations are periodic, and whether they are related to the optical spectral variations reported in reference 9. The two images shown here are SWP 14597 (upper) and 14665 (lower).

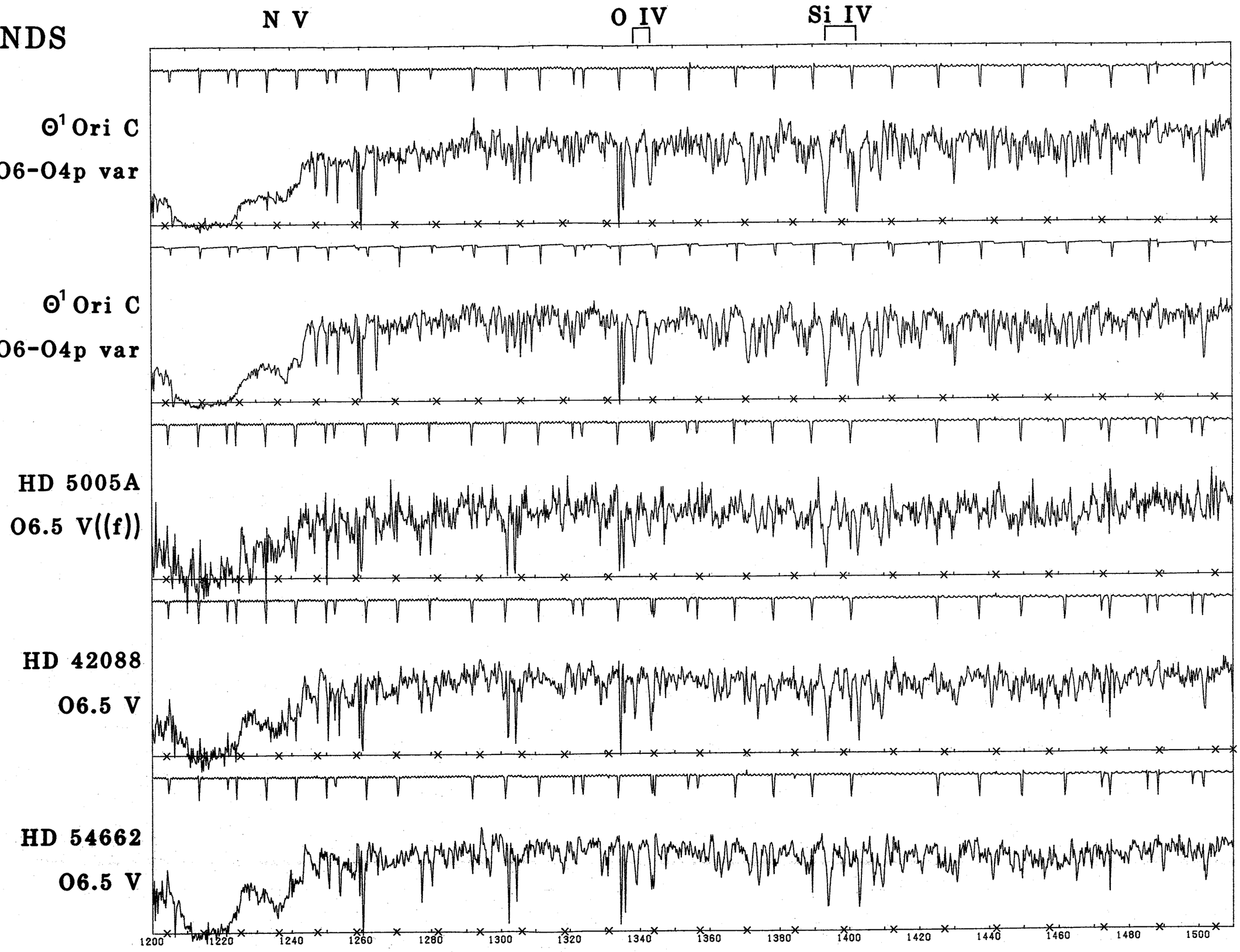

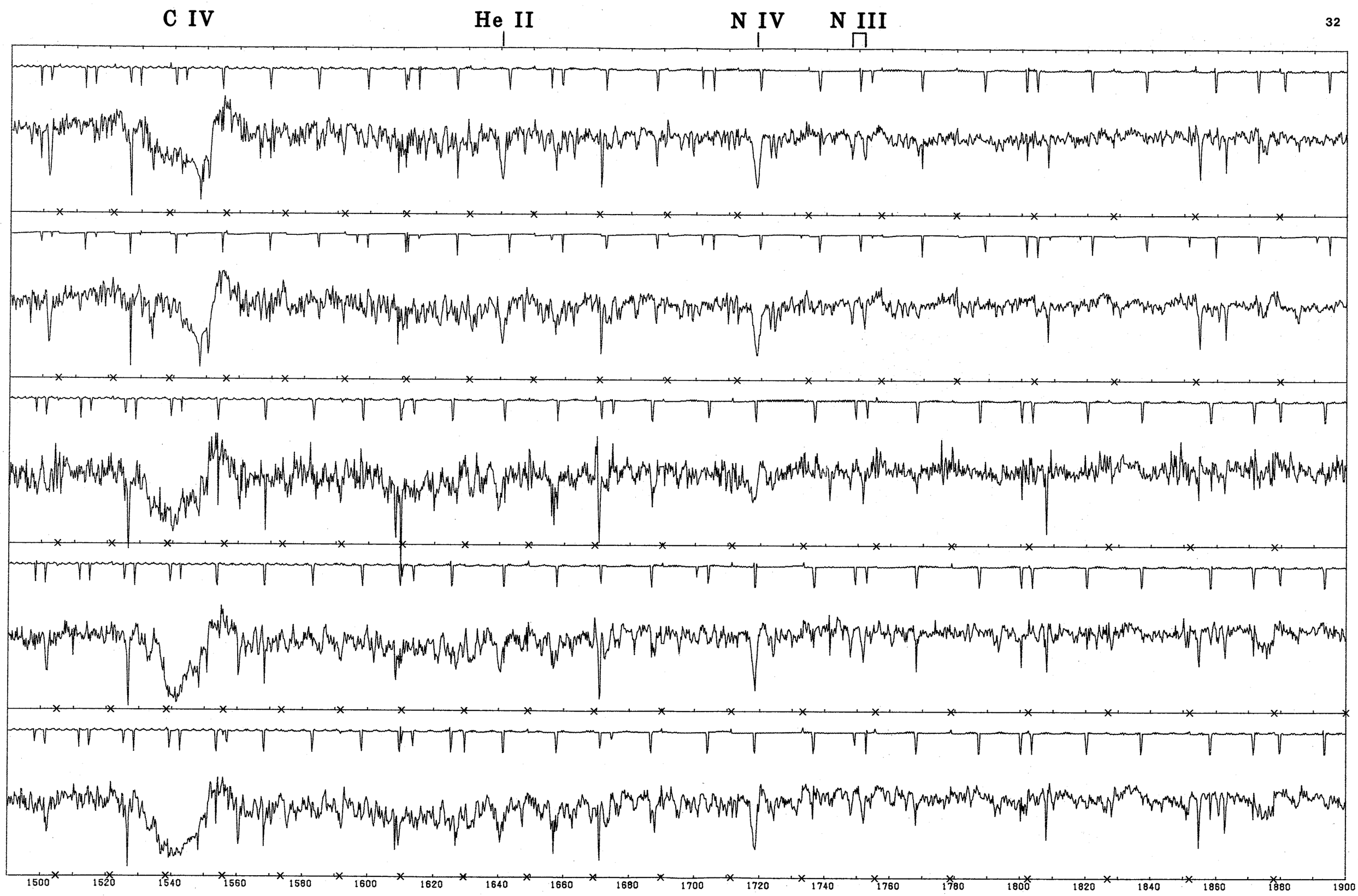
C IV
He II
N IV
N III
1500
1520
1540
1560
1580
1600
1620
1640
1660
1680
1700
1720
1740
1760
1780
1800
1820
1840
1860
1880
1900

PECULIAR DWARFS

HD 49798 is a well known nitrogen-rich, carbon-deficient subdwarf which has been analyzed by Kudritzki and Simon (1978) and Hamann *et al.* (1981), and was the subject of a detailed ultraviolet line identification study by Bruhweiler, Kondo, and McCluskey (1981).

HD 39680 has a highly peculiar, variable optical spectrum (reference 4). It has weak ultraviolet P Cyg profiles for its spectral type, but extremely strong sharp, shortward wind absorption components.

HD 36879 has no known optical peculiarity other than the rapid rotation. However, it has narrow Si IV emission features which are apparently redshifted and variable, and are unique among the present sample. N IV λ1718 may have a Be-type profile. The two images are SWP 4654 (upper) and 4699 (lower), obtained 4 days apart.

The traditional spectroscopic standard τ Sco has highly unusual, enhanced stellar-wind features for its spectral type. The asymmetrical N V absorptions and the C IV P Cyg emission are stronger than those in normal O9 V spectra, while Si IV displays asymmetric absorptions which are unique among the present main-sequence sample.

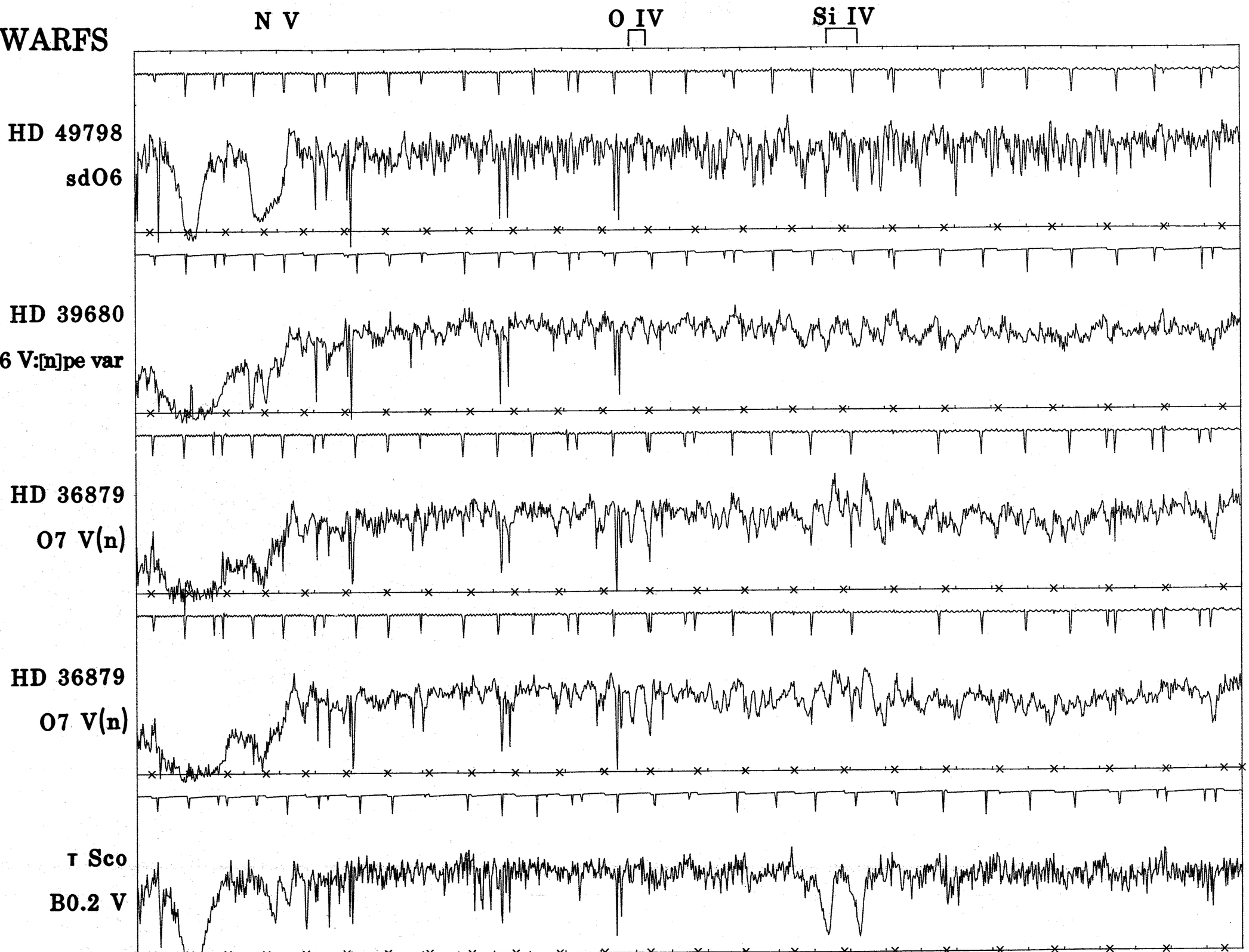

C IV He II N IV N III

1500 1520 1540 1560 1580 1600 1620 1640 1660 1680 1700 1720 1740 1760 1780 1800 1820 1840 1860 1880 1900

NITROGEN ENHANCED O8 DWARFS

The Si IV λλ1394, 1403 wind absorption trough in the spectrum of λ Ori is consistent with its optical luminosity classification as a giant (reference 3), while the absence of any Si IV wind effects in the other three spectra confirms that they are dwarfs. The blue-violet spectrum of HD 48279 shows a moderate nitrogen enhancement (reference 6).

The strength of the N V λλ1239, 1243 wind feature in HD 14633 is more similar to that in the giant than in the normal dwarf; the enhanced ultraviolet N V in HD 14633 has been discussed by Abbott, Bohlin, and Savage (1982). The most striking anomaly qualitatively in the ultraviolet spectra of both HD 14633 and 48279 is the similar, marked deficiency of their C IV λλ1548, 1551 features.

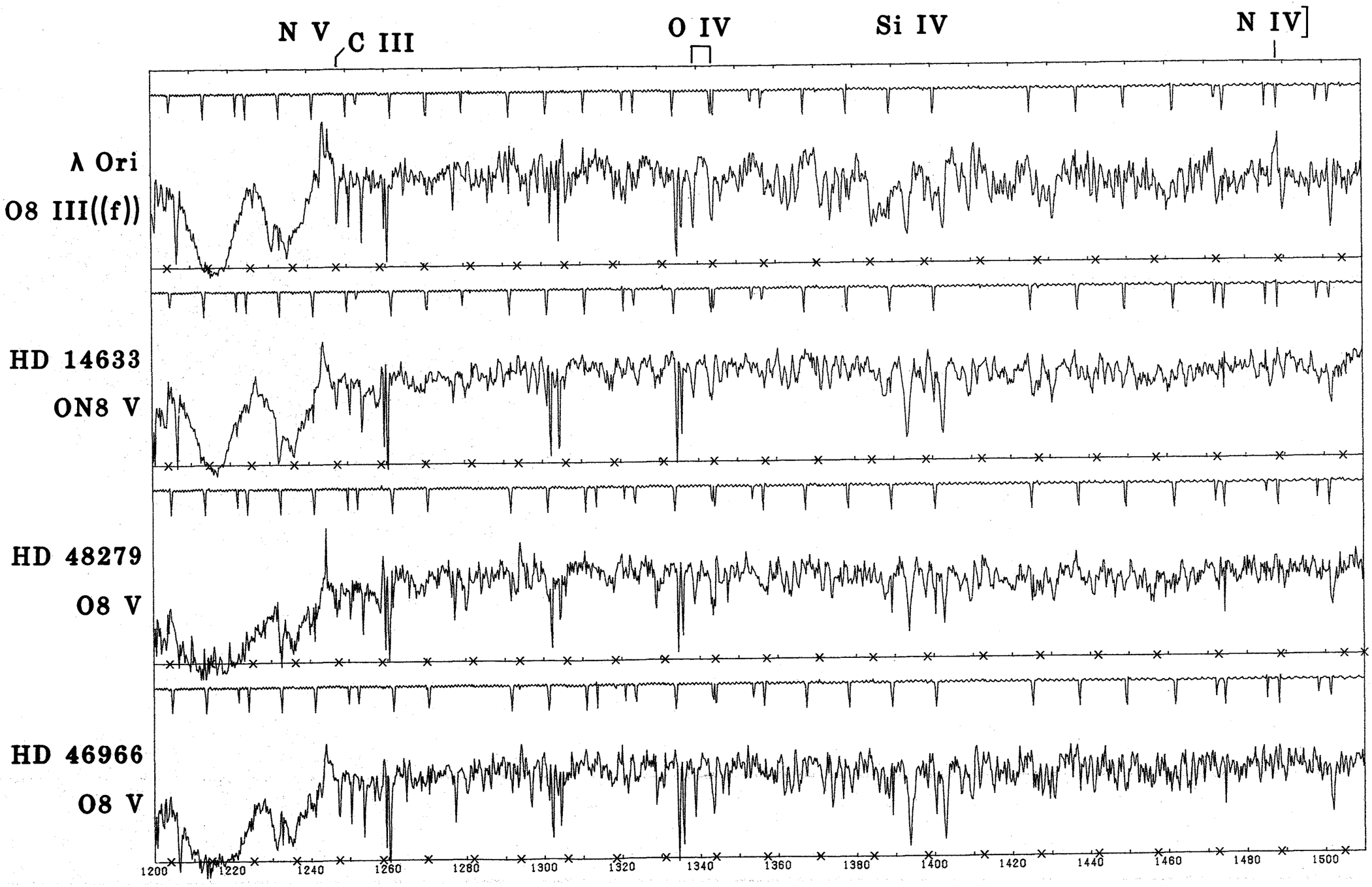

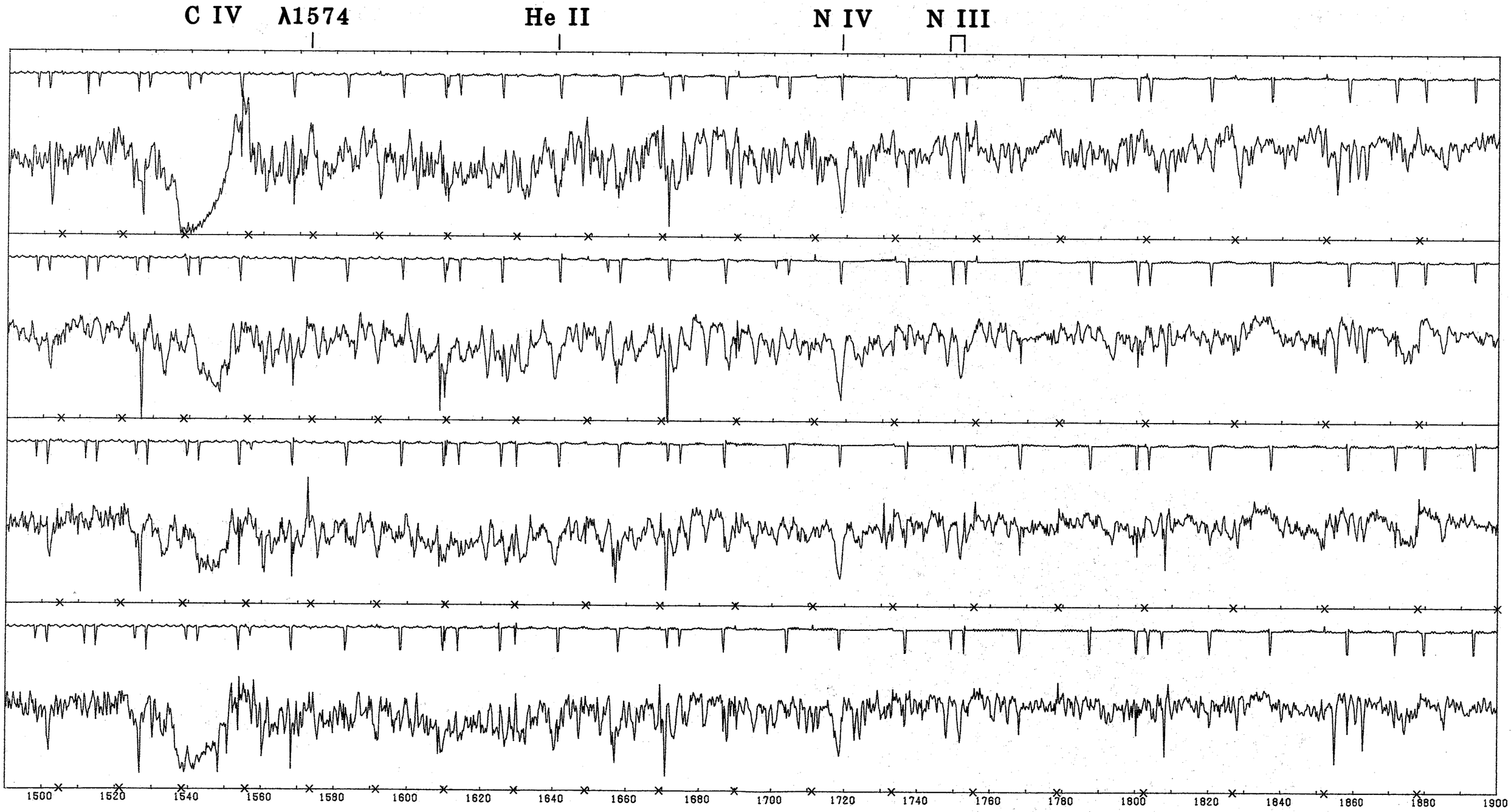
C IV λ1574
He II
N IV
N III
1500
1520
1540
1560
1580
1600
1620
1640
1660
1680
1700
1720
1740
1760
1780
1800
1820
1840
1860
1880
1900

NITROGEN ENHANCED O9 DWARFS

The behavior of Si IV λλ1394, 1403 demonstrates that HD 210809 is a supergiant, while the other three stars are dwarfs, in agreement with the optical classifications. Blue-violet spectrograms of HD 201345 and the two comparison standards are reproduced in reference 1, and a general discussion of ON spectra is given in reference 6.

N V λλ1239, 1243 shows strong, narrow, shortward wind absorption components in both ON spectra, with enhanced emission as well in HD 201345. In contrast, C IV λλ1548, 1551 is strikingly deficient in the ON spectra, and could be entirely interstellar in the case of HD 12323.

Note also the enhanced N IV] λ1486.5 emission in HD 201345, as well as the weak C III λ1247 in HD 12323.

The opposite anomalies in the N versus C features of the ON relative to the normal spectra strongly suggest an origin in abundance effects.

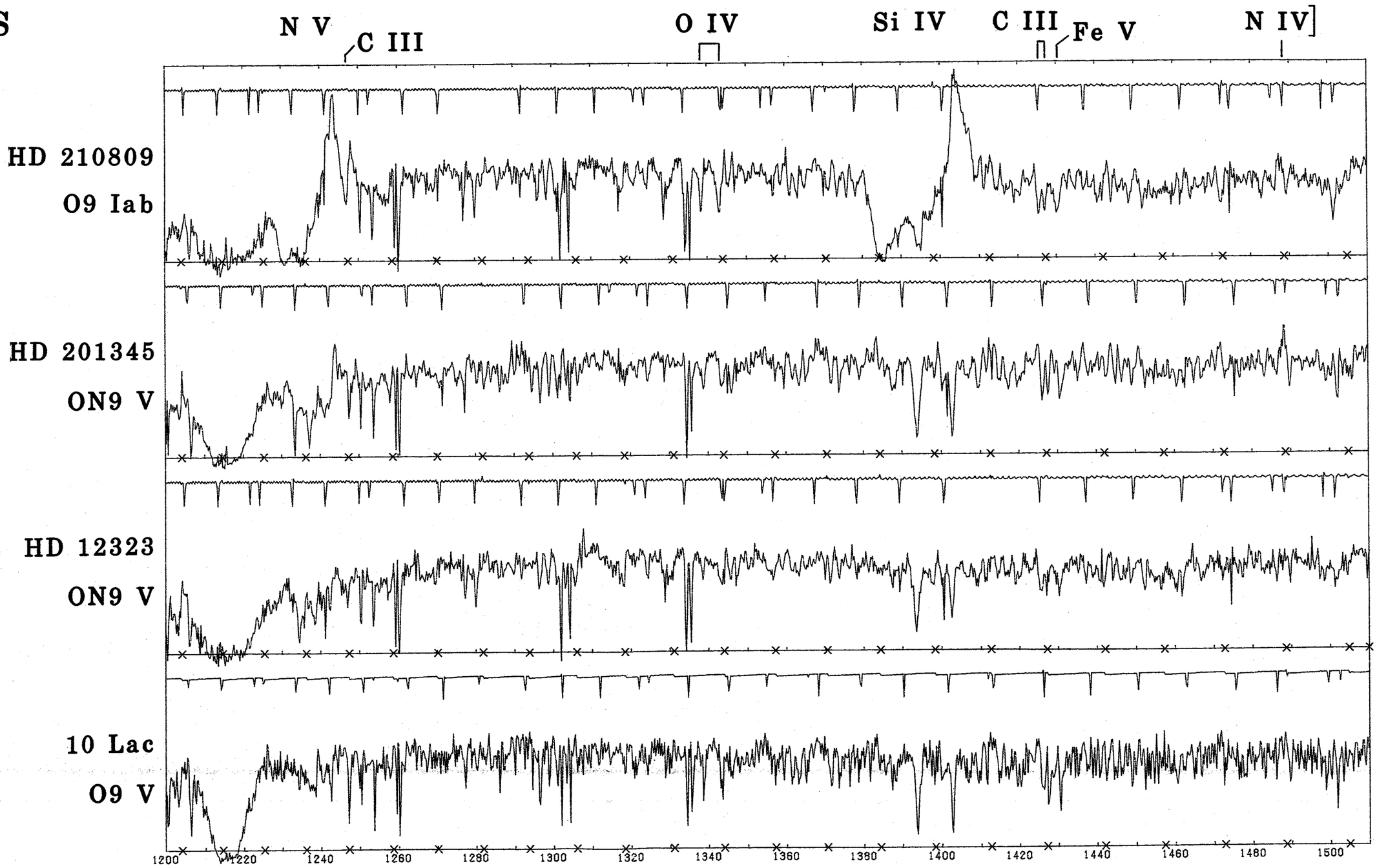

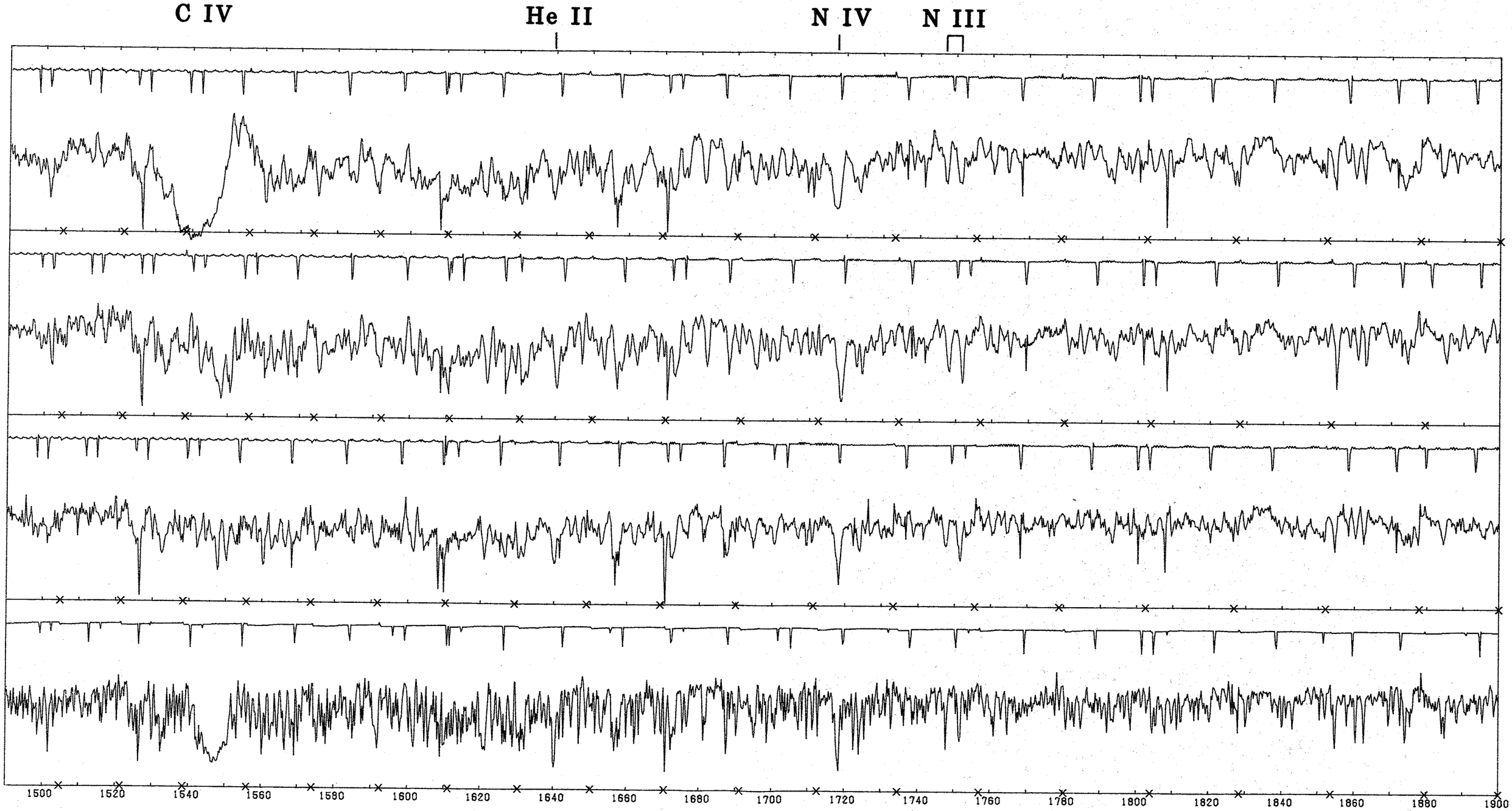
C IV
He II
N IV
N III
1500
1520
1540
1560
1580
1600
1620
1640
1660
1680
1700
1720
1740
1760
1780
1800
1820
1840
1860
1880
1900

ON/OC SUPERGIANTS

The saturated Si IV λλ1394, 1403 stellar-wind profiles confirm that all of these stars are supergiants. However, the two OC objects have very deficient N V λλ1239,1243 wind profiles, while the two ON's have weak C IV λλ1548,1551; hence, the behavior of the ultraviolet stellar-wind features shows a good correspondence to the optical absorption-line classifications (Walborn 1976). Note also the deficient C III λ1247 absorption in the two ON spectra.

HD 105056 has a lower wind terminal velocity than the other stars. Its spectrum also displays Al III λλ1855,1863 wind profiles, which are highly unusual at these spectral types.

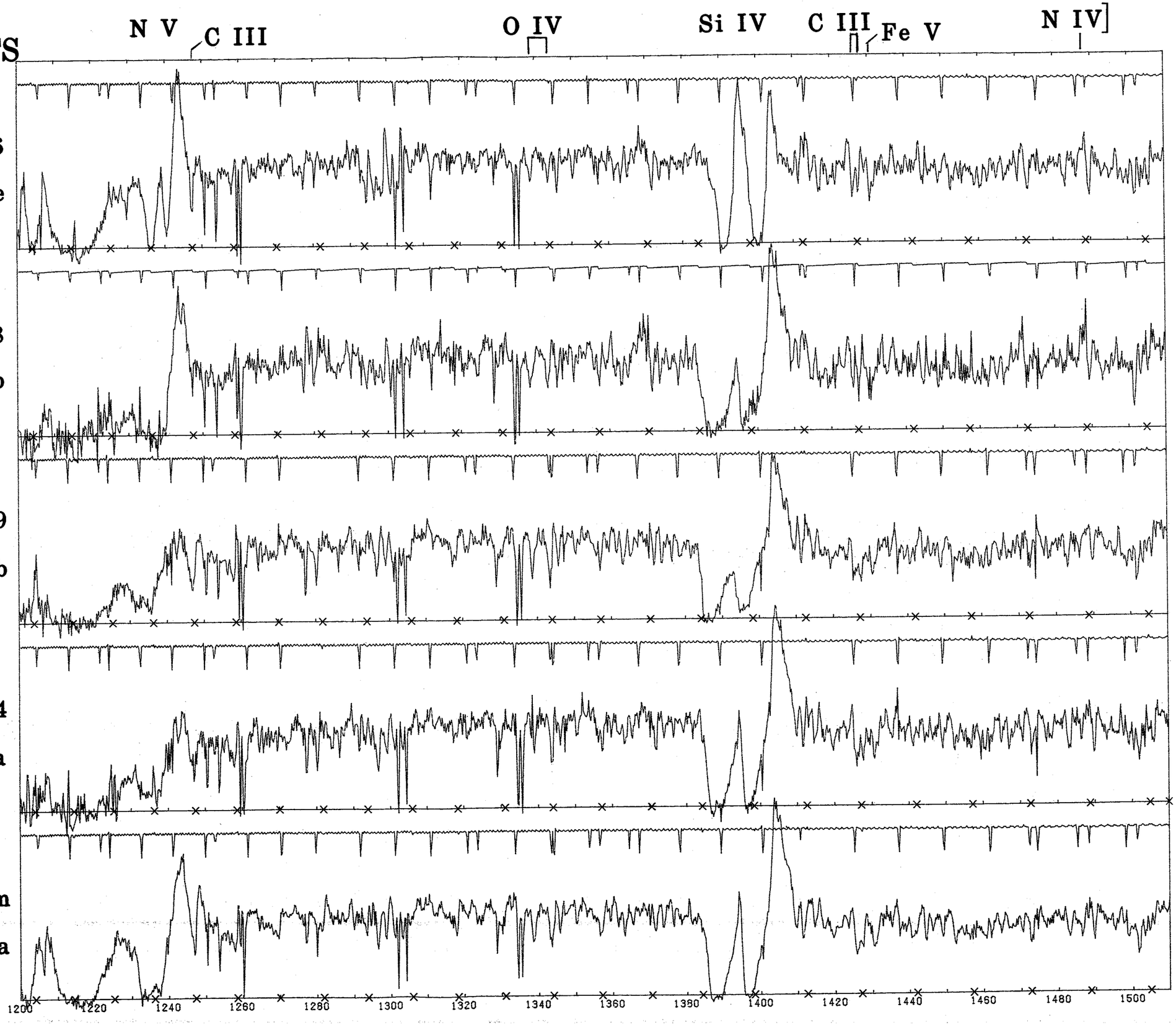

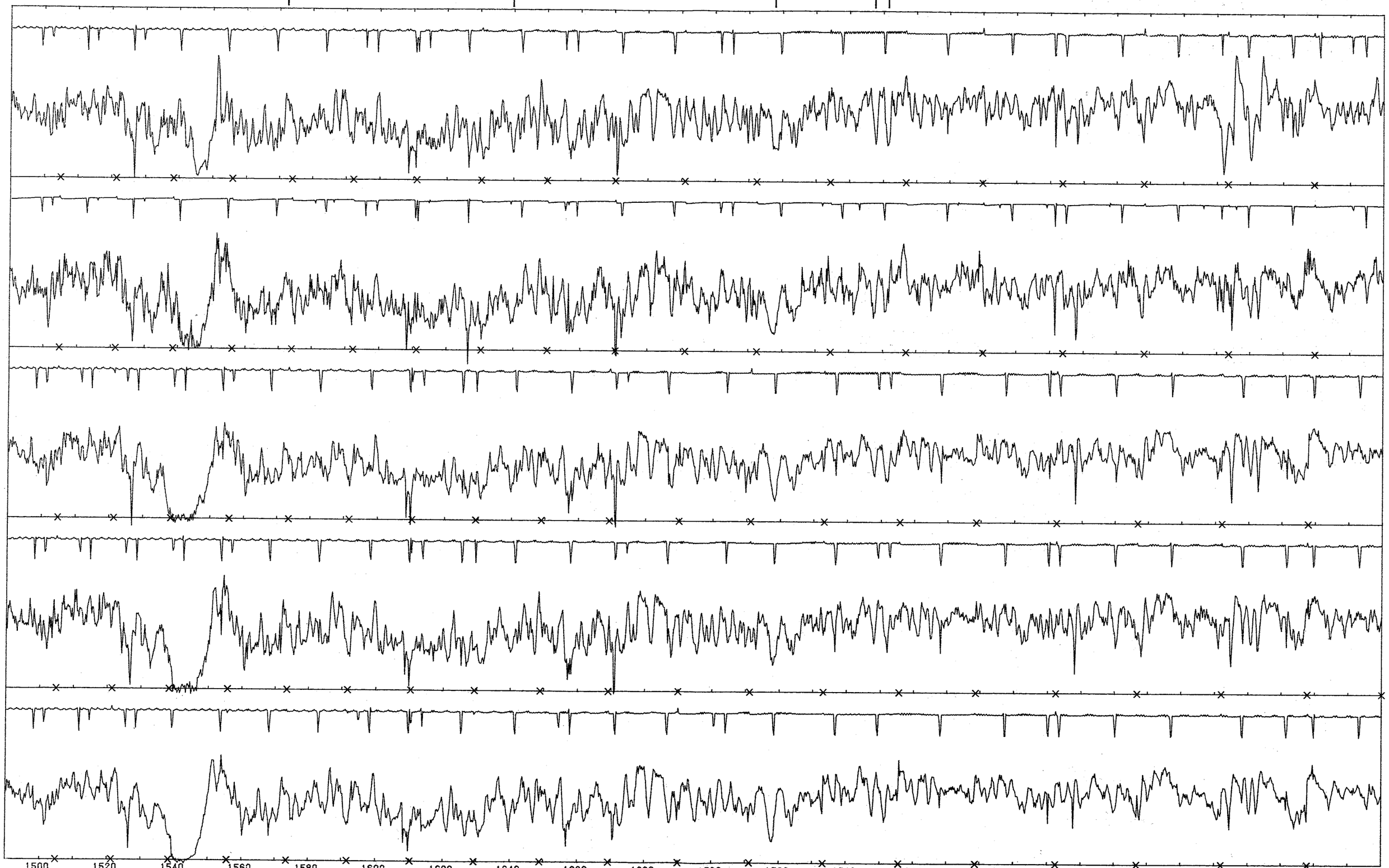
C IV
λ1574
He II
N IV
N III
Al III
1500
1520
1540
1560
1580
1600
1620
1640
1660
1680
1700
1720
1740
1760
1780
1800
1820
1840
1860
1880
1900

PECULIAR GIANTS/ SUPERGIANTS

The profiles of Si IV λλ1394, 1403 in HD 108 and 148937 show that they are not normal Of supergiants; the HD 108 profile is very peculiar while that of HD 148937 is typical of O-type giants. The Si IV profile of BD+60° 2522 indicates that it is a very luminous star. Blue-violet spectrograms of these three objects are reproduced in reference 4, and a yellow-red one of HD 148937 in reference 8.

Sanduleak 80 is a normal Of supergiant in the Small Magellanic Cloud (reference 7). The relative weakness of its Si IV profile may be due to the metal deficiency of that galaxy. (The spikes are caused by particle hits.)

HD 152408 is a luminous supergiant with enhanced mass-loss characteristics. A blue-violet spectrogram is reproduced in reference 11, and a yellow-red one in reference 8.

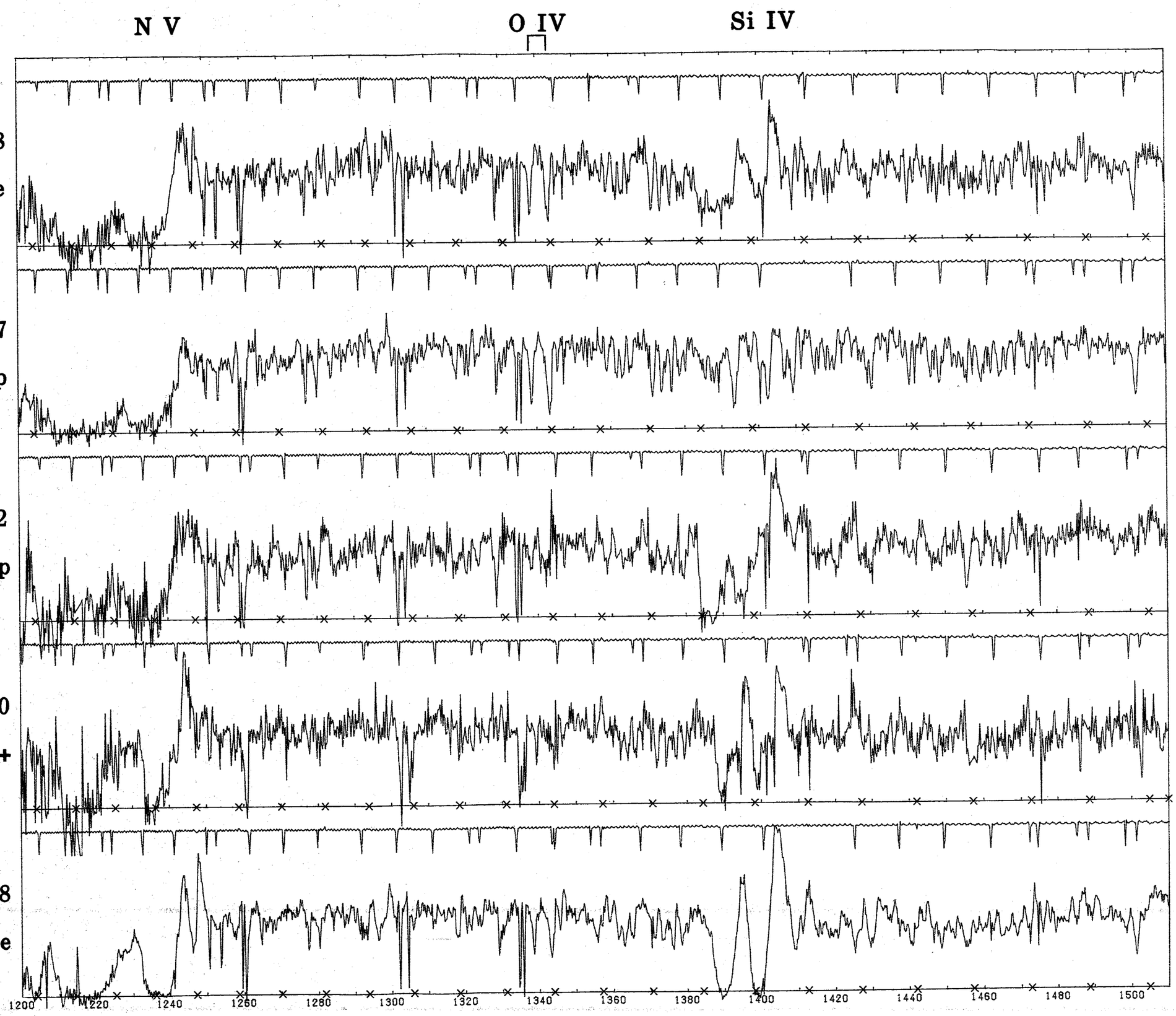

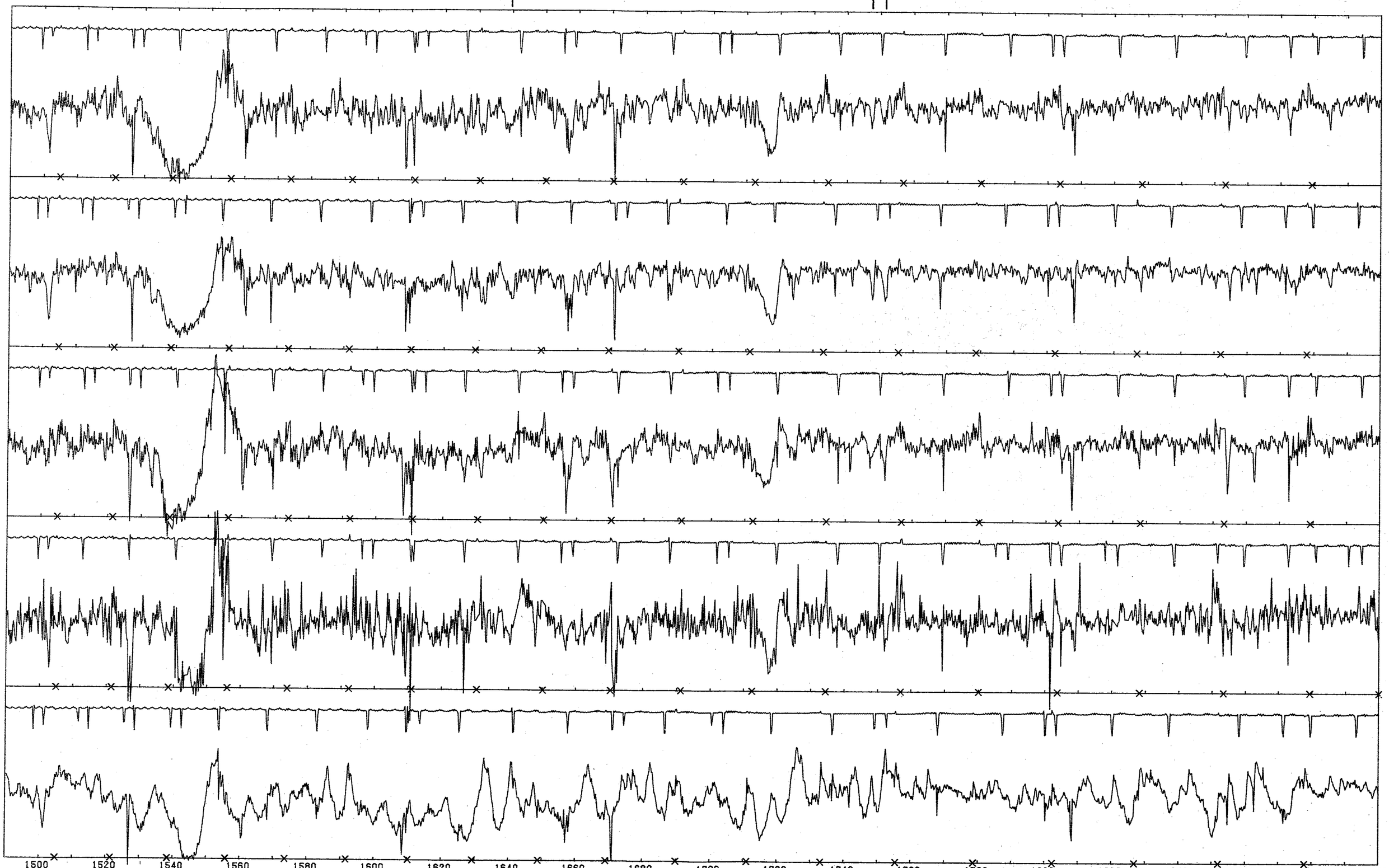
C IV
He II
N IV
N III
1500
1520
1540
1560
1580
1600
1620
1640
1660
1680
1700
1720
1740
1760
1780
1800
1820
1840
1860
1880
1900

THE WN-A STARS

The ultraviolet spectra of the WN-A stars bear evident relationships to the O3 If*, as is also the case in the blue-violet region (Walborn 1974).

N V λλ1239,1243 and C IV λλ1548, 1551 have saturated P Cyg profiles similar to those of the Of stars.

Si IV λλ1394, 1403 has a peculiar wind profile with saturated shortward absorption troughs but relatively weak emission.

He II λ1640 and N IV λ1718 have developed much stronger wind profiles than in the Of spectra, but in contrast to the Si IV, they have unsaturated absorption and very strong emission.

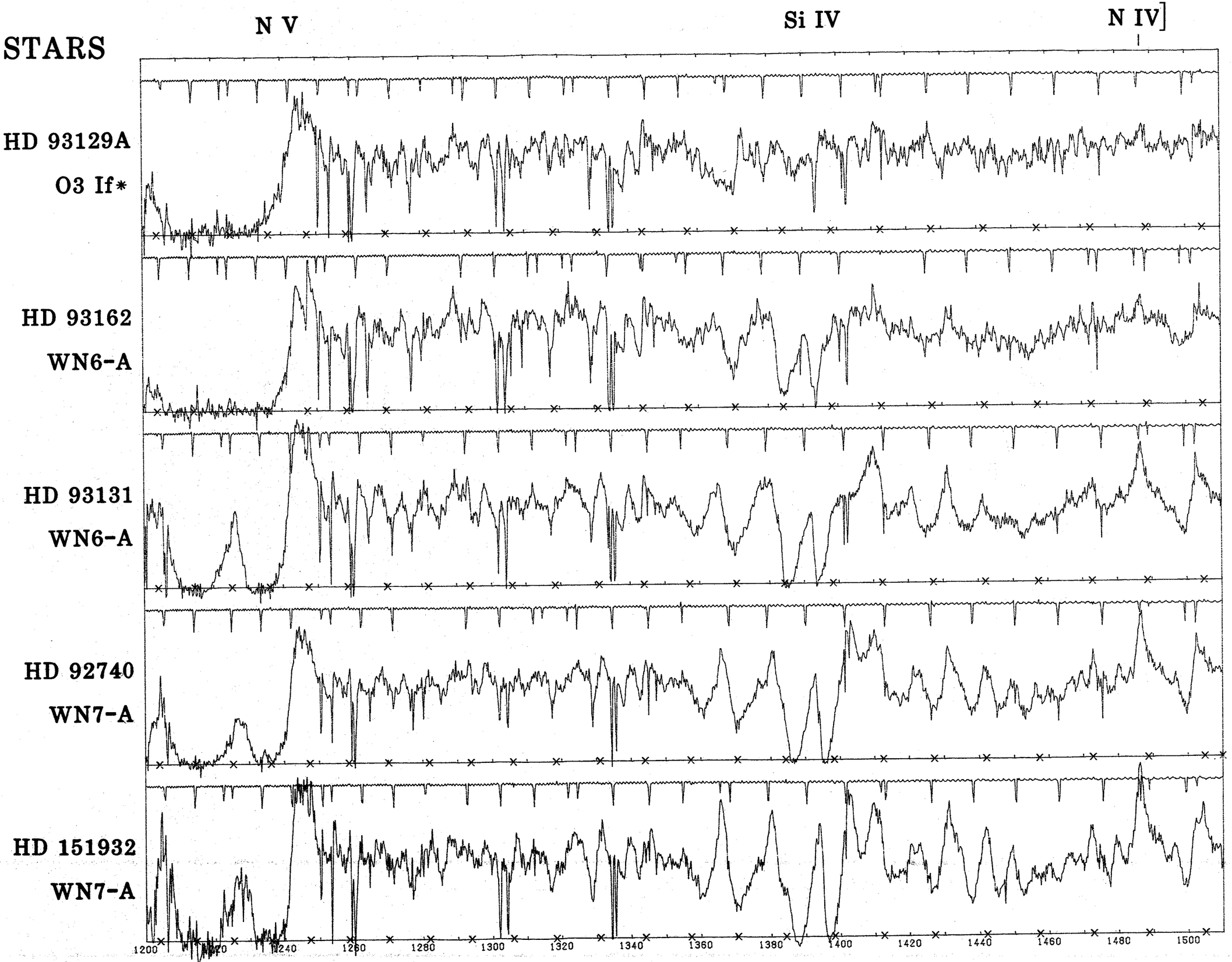

C IV He II N IV

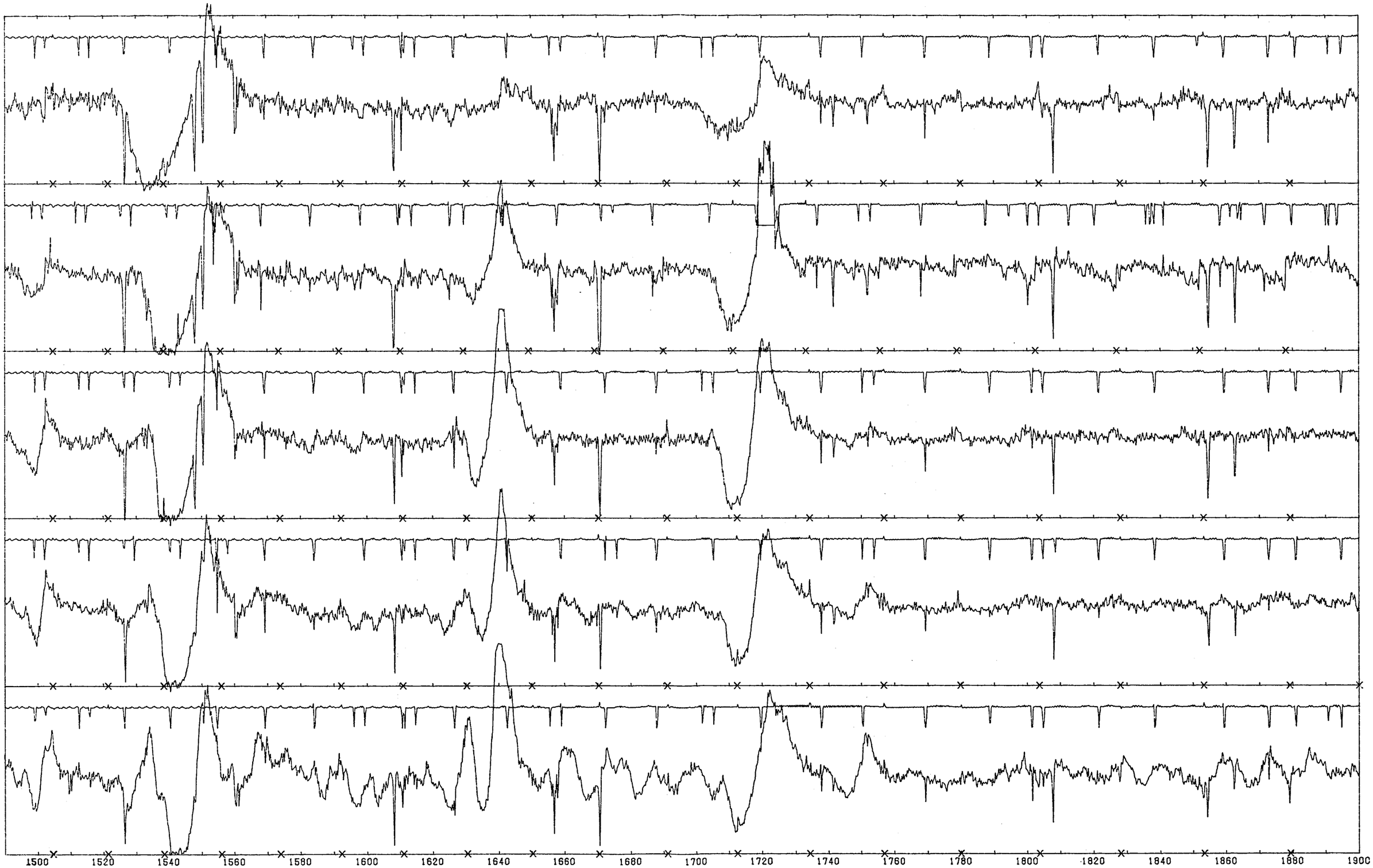
1500
1520
1540
1560
1580
1600
1620
1640
1660
1680
1700
1720
1740
1760
1780
1800
1820
1840
1860
1880
1900

1. Report No. NASA RP-1155	2. Government Accession No.	3. Recipient's Catalog No.
4. Title and Subtitle International Ultraviolet Explorer Atlas of O-Type Spectra From 1200 to 1900 Å		5. Report Date December 1985 6. Performing Organization Code 680
7. Author(s) Nolan R. Walborn, Joy Nichols-Bohlin, and Robert J. Panek		8. Performing Organization Report No. 10. Work Unit No.
9. Performing Organization Name and Address Laboratory for Astronomy and Solar Physics Goddard Space Flight Center Greenbelt, Maryland 20771		11. Contract or Grant No. 13. Type of Report and Period Covered Reference Publication
12. Sponsoring Agency Name and Address National Aeronautics and Space Administration Washington, D.C. 20546		14. Sponsoring Agency Code

15. Supplementary Notes

Nolan R. Walborn and Joy Nichols-Bohlin: Space Telescope Science Institute, Baltimore, Maryland.
Robert J. Panek: Raytheon Company and Wellesley College, Cambridge, Massachusetts.

16. Abstract

The IUE archives provide an unprecedented sample of uniform, high-quality ultraviolet stellar spectra. In particular, they contain high-resolution SWP data for nearly 200 different O stars. We have undertaken a survey of the 1200–1900 A region in about 120 of them having homogeneous optical spectral classifications, to investigate systematically the behavior of the ultraviolet features, including the prominent stellar wind profiles, and the degree to which they correlate with the optical types. The standard extracted spectrograms have been rebinned to a constant wavelength resolution of 0.25A and uniformly normalized (not dereddened) at the GSFC RDAF. They are then plotted at 10A/cm, with reseau, photometric quality, and echelle order junction flags available. This atlas contains such plots for about 100 stars, arranged in spectral-type, luminosity, and peculiar object sequences.

The results show a high degree of correlation between the ultraviolet features, both photospheric and stellar-wind, and the optical classifications for the majority of the O-type stars.

17. Key Words (Suggested by Author(s))	18. Distribution Statement
IUE, spectroscopy, O-type stars, ultraviolet, stellar winds, stellar classification	Unclassified - Unlimited Subject Category 90

19. Security Classif. (of this report)	20. Security Classif. (of this page)	21. No. of Pages	22. Price
Unclassified	Unclassified	52	A03

N-305

For sale by the National Technical Information Service, Springfield, Virginia 22161

☆U.S. GOVERNMENT PRINTING OFFICE : 1985—625-640/E1004